

A review of univariate and multivariate multifractal analysis illustrated by the analysis of marathon runners physiological data

Stéphane Jaffard*, Guillaume Saës†, Wejdene Ben Nasr‡,
Florent Palacin §, Véronique Billat¶

Abstract: We review the central results concerning wavelet methods in multifractal analysis, which consists in analysis of the pointwise singularities of a signal, and we describe its recent extension to multivariate multifractal analysis, which deals with the joint analysis of several signals; we focus on the mathematical questions that this new techniques motivate. We illustrate these methods by an application to data recorded on marathon runners.

Keywords: *Scaling, Scale Invariance, Fractal, Multifractal, Hausdorff dimension, Hölder regularity, Multivariate analysis, Wavelet, Wavelet Leader, p-leader, Multifractal Spectrum, physiological data, heartbeat frequency, Marathon races.*

*Address: Laboratoire d'Analyse et de Mathématiques Appliquées, CNRS, UMR 8050, UPEC, Créteil, France jaffard@u-pec.fr

†Address: Laboratoire d'Analyse et de Mathématiques Appliquées, CNRS, UMR 8050, UPEC, Créteil, France and Département de Mathématique, Université de Mons, Place du Parc 20, 7000 Mons (Belgium) guillaume.saes@u-pec.fr

‡Address: Laboratoire d'Analyse et de Mathématiques Appliquées, CNRS, UMR 8050, UPEC, Créteil, France wejdene.nasr@u-pec.fr

§Laboratoire de neurophysiologie et de biomécanique du mouvement, Institut des neurosciences de l'Université Libre de Bruxelles, Belgium palacinflorent@gmail.com

¶Université Paris-Saclay, Univ Evry, F-91000 Evry-Courcouronnes, France. veronique.billat@billatraining.com

Contents

1	Introduction	3
2	Univariate multifractal analysis	7
2.1	The multifractal spectrum	7
2.2	Alternative formulations of the multifractal formalism	9
2.3	Pointwise exponents	11
2.4	Orthonormal wavelet decompositions	13
2.5	Wavelet pointwise regularity characterizations	16
2.6	Towards a classification of pointwise singularities	19
2.7	Mathematical results concerning the multifractal formalism	24
2.8	Generic results	29
2.9	Implications on the analysis of marathon runners data	30
3	Multivariate multifractal analysis	34
3.1	Multivariate spectrum	34
3.2	Probabilistic interpretation of scaling functions	36
3.3	Multivariate multifractal formalism	37
3.4	Fractional Brownian motions in multifractal time	43
3.5	Multivariate analysis of marathon physiological data	47
4	Conclusion	48

1 Introduction

Everywhere irregular signals are ubiquitous in nature: Classical examples are supplied by natural phenomena (hydrodynamic turbulence [90], geophysics, natural textures [78]), physiological data (medical imaging [12], heartbeat intervals [5], E.E.G [39]); they are also present in human activity and technology (finance [18], internet traffic [3], repartition of population [48, 109], text analysis [86], art [7]). The analysis of such phenomena requires the modelling by everywhere irregular functions, and it is therefore natural to use mathematical regularity parameters in order to classify such data, and to study mathematical models which would fit their behavior. Constructing and understanding the properties of such functions has been a major challenge in mathematical analysis for a long time: Shortly after Cauchy gave the proper definition of a continuous function, the question of determining if a continuous function is necessarily differentiable at some points was a major issue for a large part of the 19th century; though a first counterexample was found by Bolzano, his construction remained unknown from the mathematical community, and it was only in 1872, with the famous Weierstrass functions

$$\mathcal{W}_{a,\omega}(x) = \sum_{n=0}^{+\infty} \frac{\sin(a^n x)}{a^{\omega n}} \quad \text{for } a > 1 \quad \text{and} \quad \omega \in (0, 1), \quad (1)$$

that the problem was settled. However, such constructions were considered as weird counterexamples, and not representative of what is commonly met, both in mathematics and in applications. In 1893, Charles Hermite wrote to Thomas Stieltjes: *I turn my back with fright and horror to this lamentable plague: continuous functions without derivative.* The first statement that smooth or piecewise smooth functions were not adequate for modelling natural phenomena but were rather exceptional came from physicists, see e.g. the introduction of the famous book of Jean Perrin “Les atomes”, published in 1913. On the mathematical side, the evolution was slow: In 1931, Mazurkiewicz and Banach showed that most continuous functions are nowhere differentiable (“most” meaning here that such functions form a residual set in the sense of Baire categories). This spectacular result changed the perspective: Functions which were considered as exceptional and rather pathological actually were the common rule, and smooth functions turn out to be exceptional.

A first purpose of multifractal analysis is to supply mathematical notions which allow to quantify the irregularity of functions, and therefore yield quantitative tools that can be applied to real life data in order to determine if they fit a given model, and, if it is the case, to determine the correct parameters of the model. One can also be more ambitious and wonder which “types” of singularities are present in the data, which may yield an important information of the nature of the signal; a typical example is supplied by *chirps* which are singularities which behave like

$$g(x) = |x - x_0|^\alpha \cos \left(\frac{1}{|x - x_0|^\beta} \right), \quad (2)$$

displaying fast oscillations near the singularity at x_0 . Such singularities are e.g. predicted by some models of turbulence and therefore determining if they can be found in the recorded

data in wind tunnels is an important issue in the understanding of the physical nature of turbulence.

A first step in this program was performed by A. Kolmogorov in 1941 [82]. Let $f : \mathbb{R}^d \rightarrow \mathbb{R}$. The *Kolmogorov scaling function* of f is the function $\eta_f(p)$ implicitly defined by

$$\forall p > 0, \quad \int |f(x+h) - f(x)|^p dx \sim |h|^{\eta_f(p)}, \quad (3)$$

the symbol \sim meaning that

$$\eta_f(p) = \liminf_{|h| \rightarrow 0} \frac{\log \left(\int |f(x+h) - f(x)|^p dx \right)}{\log |h|}. \quad (4)$$

Note that, if f is smooth, then one has to use differences of order 2 or more in order to define correctly the scaling function. Kolmogorov proposed to use this tool as a way to determine if some simple stochastic processes are fitted to model the velocity of turbulent fluids at small scales, and a first success of this approach was that fractional Brownian motions (see Section 2.2) do not yield correct models (their scaling functions are linear, whereas the one measured on turbulent flows are significantly concave [11]).

An important interpretation of the Kolmogorov scaling function can be given in terms of *global smoothness* indices in families of functions spaces: the spaces $\text{Lip}(s, L^p(\mathbb{R}^d))$ defined as follows. Let $s \in (0, 1)$, and $p \in [1, \infty]$; $f \in \text{Lip}(s, L^p(\mathbb{R}^d))$ if $f \in L^p(\mathbb{R}^d)$ and

$$\exists C > 0, \quad \forall h > 0, \quad \int |f(x+h) - f(x)|^p dx \leq C|h|^{sp} \quad (5)$$

(here also, larger smoothness indices s are reached by replacing the first-order difference $|f(x+h) - f(x)|$ by higher order differences). It follows from (3) and (5) that,

$$\forall p \geq 1, \quad \eta_f(p) = p \cdot \sup\{s : f \in \text{Lip}(s, L^p(\mathbb{R}^d))\}. \quad (6)$$

An alternative formulation of the scaling function can be given in terms of global regularity indices supplied by Sobolev spaces, the definition of which we now recall.

Definition 1 Let $s \in \mathbb{R}$ and $p \geq 1$. A function f belongs to the Sobolev space $L^{p,s}(\mathbb{R}^d)$ if $(Id - \Delta)^{s/2} f \in L^p$, where $g = (Id - \Delta)^{s/2} f$ is defined through its Fourier transform as

$$\hat{g}(\xi) = (1 + |\xi|^2)^{s/2} \hat{f}(\xi).$$

This definition amounts to state that the fractional derivative of f of order s belongs to L^p . The classical embeddings between the Sobolev and the $\text{Lip}(s, L^p)$ spaces imply that

$$\forall p \geq 1, \quad \eta_f(p) = p \cdot \sup\{s : f \in L^{p,s}(\mathbb{R}^d)\}. \quad (7)$$

In other words, the scaling function tells, for each p , the order of (fractional) derivation of f up to which $f^{(s)}$ belongs to L^p .

A limitation of the use of the Kolmogorov scaling function for classification purposes is that many models display almost identical scaling functions (a typical example is supplied by the velocity of fully developed turbulence, see e.g. [99, 84]); the next challenge therefore is to construct alternative scaling functions which would allow to draw distinctions between such models. A major advance in this direction was reached in 1985 when Uriel Frisch and Giorgio Parisi proposed another interpretation of the scaling function in terms of *pointwise singularities* of the data [100]. In order to state their assertion, we first need the recall the most commonly used notion of pointwise regularity.

Definition 2 *Let $f : \mathbb{R}^d \rightarrow \mathbb{R}$ be a locally bounded function, $x_0 \in \mathbb{R}^d$ and let $\gamma \geq 0$; f belongs to $C^\gamma(x_0)$ if there exist $C > 0$, $R > 0$ and a polynomial P of degree less than γ such that*

$$\text{if } |x - x_0| \leq R, \quad \text{then} \quad |f(x) - P(x - x_0)| \leq C|x - x_0|^\gamma.$$

The Hölder exponent of f at x_0 is

$$h_f(x_0) = \sup \{ \gamma : f \text{ is } C^\gamma(x_0) \}. \quad (8)$$

Some functions have a very simple Hölder exponent. For instance, the Hölder exponent of the Weierstrass functions $\mathcal{W}_{a,\omega}$ is constant and equal to ω at every point (such functions are referred to as *monohölder functions*); since $\omega < 1$ we thus recover the fact that $\mathcal{W}_{a,\omega}$ is nowhere differentiable. However, the Hölder exponent of other functions turn out to be extremely irregular, and U. Frisch and G. Parisi introduced the *multifractal spectrum* \mathcal{D}_f as a new quantity which allows to quantify some of its properties: $\mathcal{D}_f(H)$ denotes the fractional dimension of the *isoregularity sets*, i.e. the sets

$$\{x : h_f(x) = H\}. \quad (9)$$

Based on statistical physics arguments, they proposed the following relationship between the scaling function and $\mathcal{D}_f(H)$:

$$\mathcal{D}_f(H) = \inf_p (d + Hp - \eta_f(p)), \quad (10)$$

which is referred to as the *multifractal formalism*, see [100] (we will discuss in Section 2.1 the “right” notion of fractional dimension needed here). Though the remarkable intuition which lies behind this formula proved extremely fruitful, it needs to be improved in order to be completely effective; indeed many natural processes used in signal or image modelling do not follow this formula if one tries to extend it to negative values of p , see [83]; additionally, the only mathematical result relating the spectrum of singularities and the Kolmogorov scaling function in all generality is very partial, see [57, 62]. In Section 2.2 we will discuss (10), and see how it needs to be reformulated in terms of wavelet expansions in order to reach a fairly general level of validity. In Section 2.3 we will discuss the relevance of the Hölder exponent (8) and introduce alternative exponents which are better fitted to the analysis of large classes of real-life data. Their characterization requires the introduction of orthonormal wavelet bases. This tool and its relevance for global regularity is recalled in Section 2.4 and

the characterizations of pointwise regularity which they allow are performed in Section 2.5. This leads to a classification of pointwise singularities which yields a precise description of the oscillations of the function in the neighbourhood of its singularities which is developed in Section 2.6. This implications of this classification on the different formulations of the multifractal formalism are developed in Section 2.7. The tools thus developed are applied to marathon runners physiological data (heart rate, acceleration, cadence, i.e. number of steps per minute) in Section 2.9; thus showing that they lead to a sharper analysis of the physiological modifications during the race. The numerical results derived on real-life data have been obtained using the Wavelet p -Leader and Bootstrap based MultiFractal analysis (PLBMF) toolbox available on-line at

<https://www.irit.fr/Herwig.Wendt/software.html>

The explosion of data sciences recently made available collections of signals the singularities of which are expected to be related in some way; typical examples are supplied by EEG collected at different areas of the brain, or by collections of stock exchange prizes. The purpose of Section 3 is to address the extension of multifractal analysis to the multivariate setting, i.e. to several functions. In such situations, a pointwise regularity exponent $h_i(x)$ is associated with each signal $f_i(x)$ and the challenge is to recover the *joint multivariate spectrum* of the f_i which is defined as the fractional dimension of the sets of points x where each of the exponents $h_i(x)$ takes a given value: If m signals are available, we define

$$E_{f_1, \dots, f_m}(H_1, \dots, H_m) = \{x : h_1(x) = H_1, \dots, h_m(x) = H_m\}, \quad (11)$$

and the *joint multifractal spectrum* is

$$D_{f_1, \dots, f_m}(H_1, \dots, H_m) = \dim(E_{f_1, \dots, f_m}(H_1, \dots, H_m)). \quad (12)$$

These notions were introduced by C. Meneveau *et al.* in the seminal paper [96] which addressed the joint analysis of the dissipation rate of kinetic energy and passive scalar fluctuations for fully developed turbulence, and a general abstract setting was proposed by J. Peyrière in [101]; In Section 3.1, we introduce the mathematical concepts which are relevant to this study. In Section 3.2 we give a probabilistic interpretation of the scaling functions introduced in Section 2, and we show how they naturally lead to a 2-variable extension in terms of correlations. The initial formulation of the multifractal formalisms based on extensions of the Kolmogorov scaling function suffers from the same drawbacks as in the univariate case. This leads naturally to a reformulation of the multifractal formalism which is examined in Section 3.3, where we also investigate the additional advantages supplied by multivariate multifractal analysis for singularity classifications. In order to investigate its relevance, we study a toy-example which is supplied by Brownian motions in multifractal time in Section 3.4. In Section 3.5, we illustrate the mathematical results thus collected by applications to the joint analysis of heartbeat, cadence and acceleration of marathon runners.

2 Univariate multifractal analysis

2.1 The multifractal spectrum

In order to illustrate the motivations of multifractal analysis, let us come back to the initial problem we mentioned: How badly can a continuous function behave? We mentioned the surprising result of Mazurkiewicz and Banach stating that a generic continuous function is nowhere differentiable, and the Weierstrass functions yield examples of continuous functions which may have an arbitrarily small (and constant) Hölder exponent. This can actually be improved: A generic continuous function satisfies

$$\forall x \in \mathbb{R}, \quad h_f(x) = 0, \quad (13)$$

see [17]: At every point the Hölder exponent of f is as bad as possible. An example of such a continuous function is supplied by a slight variant of Weierstrass functions:

$$f(x) = \sum_{j=1}^{\infty} \frac{1}{j^2} \sin(2^j x).$$

Let us now consider a different functional setting: Let $f : [0, 1] \rightarrow [0, 1]$ be an increasing function. At any given point $x \in [0, 1]$ f can have a discontinuity at x , in which case $h_f(x) = 0$. Nonetheless, this worse possible behavior cannot be met everywhere: An important theorem of Lebesgue states that f is almost everywhere differentiable and therefore satisfies

$$\text{for almost every } x \in [0, 1], \quad h_f(x) \geq 1.$$

The global regularity assumption (the fact that f is increasing implies that its derivative in the sense of distributions is a bounded Radon measure) implies that, in sharp contradistinction with generic continuous functions, the set of points such that $h_f(x) < 1$ is “small” (its Lebesgue measure vanishes). On other hand, the set of points where it is discontinuous can be an arbitrary countable set (but one easily checks that it cannot be larger). What can we say about the size the sets of points with intermediate regularity (i.e. having Hölder exponents between 0 and 1), beyond the fact that they have a vanishing Lebesgue measure? Answering this problem requires to use some appropriate notion of “size” which allows to draw differences between sets of vanishing Lebesgue measure. The right mathematical notion fitted to this problem can be guessed using the following argument. Let

$$E_f^\alpha = \{x : f \notin C^\alpha(x)\}.$$

Clearly, if $x \in E_f^\alpha$, then there exists a sequence of dyadic intervals

$$\lambda_{j,k} = \left[\frac{k}{2^j}, \frac{k+1}{2^j} \right] \quad (14)$$

such that

- x belongs either to $\lambda_{j,k}$ or to one of its two closest neighbours of the same width,

- the increment of f on $\lambda_{j,k}$ is larger than $2^{-\alpha j} = |\lambda_{j,k}|^\alpha$ (where $|A|$ stands for the diameter of the set A).

Let $\varepsilon > 0$, and consider the *maximal* dyadic intervals of this type of width less than $\varepsilon/3$, for all possible $x \in E_f^\alpha$, and denote this set by $\Lambda_\alpha^\varepsilon$. These intervals are disjoint (indeed two dyadic intervals are either disjoint or one is included in the other); and, since f is increasing, the increment of f on $[0, 1]$ is bounded by the sum of the increments on these intervals. Therefore

$$\sum_{\lambda \in \Lambda_\alpha^\varepsilon} |\lambda|^\alpha \leq f(1) - f(0).$$

The intervals 3λ (which consists in the dyadic interval λ and its two closest neighbours of the same length) for $\lambda \in \Lambda_\alpha^\varepsilon$ form an ε -covering of E_f^α (i.e. a covering by intervals of length at most ε), and this ε -covering satisfies

$$\sum_{\lambda \in \Lambda_\alpha^\varepsilon} |3\lambda|^\alpha = 3^\alpha \sum_{\lambda \in \Lambda_\alpha^\varepsilon} |\lambda|^\alpha \leq f(1) - f(0).$$

This property can be interpreted as stating that the α -dimensional Hausdorff measure of E_f^α is finite; we now give a precise definition of this notion.

Definition 3 Let A be a subset of \mathbb{R}^d . If $\varepsilon > 0$ and $\delta \in [0, d]$, let

$$M_\varepsilon^\delta = \inf_R \left(\sum_i |A_i|^\delta \right),$$

where R is an ε -covering of A , i.e. a covering of A by bounded sets $\{A_i\}_{i \in \mathbb{N}}$ of diameters $|A_i| \leq \varepsilon$ (the infimum is therefore taken on all ε -coverings). For any $\delta \in [0, d]$, the δ -dimensional Hausdorff measure of A is

$$mes_\delta(A) = \lim_{\varepsilon \rightarrow 0} M_\varepsilon^\delta.$$

One can show that there exists $\delta_0 \in [0, d]$ such that

$$\begin{cases} \forall \delta < \delta_0, & mes_\delta(A) = +\infty \\ \forall \delta > \delta_0, & mes_\delta(A) = 0. \end{cases}$$

This critical δ_0 is called the *Hausdorff dimension* of A , and is denoted by $\dim(A)$ (and an important convention is that, if A is empty, then $\dim(\emptyset) = -\infty$).

The example we just worked out shows that a global regularity information on a function yields information on the Hausdorff dimensions of its sets of Hölder singularities. This indicates that the Hausdorff dimension is the natural choice in (10), and motivates the following definition.

Definition 4 Let $f : \mathbb{R}^d \rightarrow \mathbb{R}$ be a locally bounded function. The *multifractal Hölder spectrum* of f is the function

$$\mathcal{D}_f(H) = \dim(\{x : h_f(x) = H\}),$$

where \dim denotes the Hausdorff dimension.

This definition justifies the denomination of *multifractal functions*: One typically considers functions f that have non-empty isoregularity sets (9) for H taking all values in an interval of positive length, and therefore one deals with an infinite number of fractal sets $E_f(H)$. The result we obtained thus implies that, if f is an increasing function, then

$$\mathcal{D}_f(H) \leq H. \quad (15)$$

This can be reformulated in a function space setting which puts in light the sharp contrast with (13): Indeed, recall that any function of bounded variation is the difference of an increasing and a decreasing function; we have thus obtained the following result.

Proposition 1 *Let $f : \mathbb{R} \rightarrow \mathbb{R}$ be a function of bounded variation. Then its multifractal spectrum satisfies*

$$\forall H, \quad \mathcal{D}_f(H) \leq H.$$

Remark: This result does not extend to several variables functions of bounded variation which, in general, are not locally bounded, in which case their Hölder exponent is not even well defined.

2.2 Alternative formulations of the multifractal formalism

We mentioned that (10) yields a poor estimate of the multifractal spectrum. A typical example is supplied by sample paths of *fractional Brownian motion* (referred to as fBm), a family of stochastic processes introduced by Kolmogorov [81], the importance of which was put in light for modeling by Mandelbrot and Van Ness [92]. This family is indexed by a parameter $\alpha \in (0, 1)$, and generalizes Brownian motion (which corresponds to the case $\alpha = 1/2$); fBm of index α is the only centered Gaussian random process B^α defined on \mathbb{R}^+ which satisfies

$$\forall x, y \geq 0 \quad \mathbb{E}(|B^\alpha(x) - B^\alpha(y)|^2) = |x - y|^{2\alpha}.$$

FBm plays an important role in signal processing because it supplies the most simple one parameter family of stochastic processes with stationary increments. Its sample paths are monohölder and satisfy

$$\text{a.s. } \forall x, \quad h_{B^\alpha}(x) = \alpha,$$

(see [79] (and [43] for a recent sharp analysis of the pointwise regularity of their sample paths) so that their multifractal spectrum is

$$\text{a.s. } \forall H, \quad \begin{cases} \mathcal{D}_{B^\alpha}(H) = 1 & \text{if } H = \alpha \\ = -\infty & \text{else.} \end{cases}$$

However, the right hand-side of (10) yields a different value for $H \in (\alpha, \alpha + 1]$: It coincides almost surely with the function defined by

$$\begin{cases} \mathcal{L}_{B^\alpha}(H) = \alpha + 1 - H & \text{if } H \in [\alpha, \alpha + 1] \\ = -\infty & \text{else,} \end{cases}$$

see [68, 71, 3]. This is due to the fact that the decreasing part of the spectrum is recovered from negative values of p in (10), and the corresponding integral is not well defined for negative ps , and may even diverge. It follows that sharper estimates of the multifractal spectrum require a renormalization procedure which would yield a numerically robust output for negative ps . Several methods have been proposed to solve this deadlock. They are all based on a modification of the Kolmogorov scaling function in order to incorporate the underlying intuition that it should include some pointwise regularity information. A consequence will be that they provide an extension of the scaling function to negative ps . This extra range of parameters plays a crucial role in several applications where it is required for classifications, see e.g. [99, 85] where the validation of turbulence models is considered, and for which the key values of the scaling function which are needed to draw significative differences between these models are obtained for $p < 0$.

A first method is based on the *continuous wavelet transform*, which is defined as follows. Let ψ be a *wavelet*, i.e. a well localized, smooth function with, at least, one vanishing moment. The continuous wavelet transform of a one-variable function f is

$$C_{a,b}(f) = \frac{1}{a} \int_{\mathbb{R}} f(t) \psi\left(\frac{t-b}{a}\right) dt \quad (a > 0, \quad b \in \mathbb{R}); \quad (16)$$

Alain Arneodo, Emmanuel Bacry and Jean-François Muzy proposed to replace, in the integral (3), the increments $|f(x+\delta) - f(x)|$ at scale δ by the continuous wavelet transform $C_{a,b}(f)$ for $a = \delta$ and $b = x$. This choice follows the heuristic that the continuous wavelet transform satisfies $|C_{a,b}(f)| \sim a^{h_f(x)}$ when a is small enough and $|b - x| \sim a$. Note that it is not valid in all generality, but typically fails for *oscillating singularities*, such as the chirps (2). Nonetheless Yves Meyer showed that this heuristic actually characterizes another pointwise regularity exponent, the *weak scaling exponent*, see [98]. Assuming that the data do not include oscillating singularities, the integral (3) is discretized and replaced by the more meaningful values of the continuous wavelet transform i.e. at its local maxima [10]; if we denote by b_k the points where these extrema are reached at the scale a , the integral (3) is thus replaced by the sum

$$\sum_{b_k} |C_{a,b_k}(f)|^p \sim a^{\zeta_f(p)} \quad \text{when } a \rightarrow 0, \quad (17)$$

This reformulations using the *multiresolution quantities* $|C_{a,b_k}(f)|$ yields better numerical results than when using the increments $|f(x+\delta) - f(x)|$; above all, the restriction to the local suprema is a way to bypass the small values of the increments which were the cause of the divergence of the integral (3) when p is negative. Numerical experiments consistently show that the multifractal formalism based on these quantities yields the correct spectrum for the fBm, and also for large collections of multifractal models, see [8].

Another way to obtain a numerically robust procedure in order to perform multifractal analysis is supplied by *Detrended Fluctuation Analysis* (DFA) : From the definition of the Hölder exponent, Kantelhardt et al. [80] proposed the following multiresolution quantity

based on the following local L^2 norms

$$T_{mfd}(a, k) = \left(\frac{1}{a} \sum_{i=1}^a |f(ak + i) - P_{k,a,N_P}(i)|^2 \right)^{\frac{1}{2}}, k = 1, \dots, n/a, \quad (18)$$

where n denotes the number of available samples and P_{t,a,N_P} is a polynomial of degree N_P obtained by local fit to f on portions of length proportional to a . The integral (3) is now replaced by

$$S_{mfd}(a, q) = \frac{a}{n} \sum_k^{n/a} T_{mfd}(a, k)^q \sim a^{\zeta_{mfd}(q)},$$

and the multifractal spectrum is obtained as usual through a Legendre transform of this new scaling function ζ_{mfd} , thus yielding the *multifractal detrended fluctuation analysis* (MFDFA). Note that, here again, we cannot expect the multifractal formalism based on such a formula to be fitted to the Hölder exponent: The choice of an L^2 norm in (18) is rather adapted to an alternative pointwise exponent, the 2-exponent, which is defined through local L^2 -norms, see Def. 5 (and [87] for an explanation of this interpretation). The MFDFA formalism performs satisfactorily and is commonly used in applications (cf., e.g., [52, 112]).

The methods we mentioned meet the following limitations: They cannot be tailored to a particular pointwise exponent: We saw that the WTMM is fitted to the weak-scaling exponent, and the MFDFA to the 2-exponent. They lack of theoretical foundation, and therefore the estimates that they yield on the multifractal spectrum are not backed by mathematical results. In practice, they are difficult to extend to data in two or more variables (for MFDFA, the computation of local best fit polynomials is an intricate issue). The obtention of an alternative formulation of the multifractal formalism which brings an answer to these two problems requires a detour through the notions of pointwise exponents, and their characterizations.

2.3 Pointwise exponents

At this point we need to discuss the different notions of pointwise regularity. One of the reasons is that, though Hölder regularity is by far the one which is most used in mathematics and in applications, it suffers a major limitation: Definition 2 requires f to be locally bounded. In applications, this limitation makes the Hölder exponent unfitted in many settings where modelling data by locally bounded functions is inadequate; in Section 2.4 we will give a numerically simple criterium which allows to verify if this assumption is valid, and we will see that the physiological data we analyse are typical examples for which it is not satisfied. On the mathematical side too, this notion often is not relevant. A typical example is supplied by the Riemann series defined as

$$\forall x \in \mathbb{R}, \quad \mathcal{R}_s(x) = \sum_{n=1}^{\infty} \frac{\sin(n^2 x)}{n^s}, \quad (19)$$

which, for $s > 1$, are locally bounded and turn out to be multifractal (in which case their multifractal analysis can be performed using the Hölder exponent [33, 56]), but it is no more the case if $s < 1$, in which case an alternative analysis is developed in [108] (using the p -exponent for $p = 2$, see Def. 5 below).

There exist two ways to deal with such situations. The first one consists in first regularizing the data, and then analyzing the new data thus obtained. Mathematically, this means that a *fractional integral* is performed on the data. Recall that, if f is a tempered distribution defined on \mathbb{R} , then the fractional integral of order t of f , denoted by $f^{(-t)}$ is defined as follows: Let $(Id - \Delta)^{-t/2}$ be the convolution operator which amounts to multiplying the Fourier transform of f with $(1 + |\xi|^2)^{-t/2}$. The fractional integral of order t of f is the function

$$f^{(-t)} = (Id - \Delta)^{-t/2}(f).$$

If f is large enough, then $f^{(-t)}$ is a locally bounded function, and one can consider the Hölder exponent of t (the exact condition under which this is true is that t has to be larger than the exponent h_f^{min} defined below by (25) or equivalently by (26)). This procedure presents the obvious disadvantage of not yielding a direct analysis of the data but of a smoothed version of them.

The other alternative available in order to characterize the pointwise regularity of non-locally bounded functions consists in using a weaker notion of pointwise regularity, the p -exponent, which we now recall. We define $B(x_0, r)$ as the ball of center x_0 and radius r .

Definition 5 *Let $p \geq 1$ and assume that $f \in L_{loc}^p(\mathbb{R}^d)$. Let $\alpha \in \mathbb{R}$; f belongs to $T_\alpha^p(x_0)$ if there exists a constant C and a polynomial P_{x_0} of degree less than α such that, for r small enough,*

$$\left(\frac{1}{r^d} \int_{B(x_0, r)} |f(x) - P_{x_0}(x)|^p dx \right)^{1/p} \leq Cr^\alpha. \quad (20)$$

The p -exponent of f at x_0 is

$$h_f^p(x_0) = \sup\{\alpha : f \in T_\alpha^p(x_0)\} \quad (21)$$

(the case $p = +\infty$ corresponds to the Hölder exponent).

This definition was introduced by Calderón and Zygmund in 1961 in order to obtain pointwise regularity results for the solutions of elliptic PDEs, see [37]. For our concern, it has the important property of being well defined under the assumption that $f \in L_{loc}^p$. For instance, in the case of the Riemann series (19), an immediate computation yields that they belong to L^2 if $s > 1/2$ so that, if $1/2 < s < 1$, p -exponents with $p \leq 2$ are relevant to study their regularity, in contradistinction with the Hölder exponent which won't be defined. Another example of multifractal function which is not locally bounded is supplied by Brjuno's function, which plays an important role in holomorphic dynamical systems, see [93]. Though it is nowhere locally bounded, it belongs to all L^p spaces and its multifractal analysis using p -exponents has been performed in [72]. Note that p -exponents can take values down to $-d/p$, see [74]. Therefore, they allow the use of *negative regularity exponents*, such as singularities of the form $f(x) = 1/|x - x_0|^\alpha$ for $\alpha < d/p$.

The general framework supplied by multifractal analysis now is ubiquitous in mathematical analysis and has been successfully used in a large variety of mathematical situations, using diverse notion of pointwise exponents such as pointwise regularity of probability measures [34], rates of convergence or divergence of series of functions (either trigonometric [13, 26] or wavelet [13, 36]) order of magnitude of ergodic averages [45, 46], to mention but a few.

2.4 Orthonormal wavelet decompositions

Methods based on the use of orthonormal wavelet bases follow the same motivations we previously developed, namely to construct alternative scaling functions based on multiresolution quantities which “incorporate” some pointwise regularity information. However, we will see that they allow to turn some of the limitations met by the previously listed methods, and they enjoy the following additional properties:

- numerical simplicity,
- explicit links with pointwise exponents (which, as we saw, may differ from the Hölder exponent),
- no need to construct local polynomial approximations (which is the case for DFA methods now in use),
- mathematical results hold concerning either the validity of the multifractal formalism supplied by (10) or of some appropriate extensions; such results can be valid for all functions, or for “generic” functions, in the sense of Baire categories, or for other notions of genericity.

Let us however mention an alternative technique which was proposed in [2] where multiresolution quantities based on local oscillations, such as

$$d_\lambda = \sup_{3\lambda} f(x) - \inf_{3\lambda} f(x),$$

or higher order differences such as

$$d_\lambda = \sup_{x,y \in 3\lambda} \left| f(x) + f(y) - 2f\left(\frac{x+y}{2}\right) \right|,$$

and which wouldn’t present the third problem that we mention. However, as far as we know, they haven’t been tested numerically.

One of the reasons for these remarkable properties is that (in contradistinction with other expansions, such as e.g. Fourier series) wavelet analysis allows to characterize both global and pointwise regularity by simple conditions on the moduli of the wavelet coefficients; as already mentioned, the multifractal formalism raises the question of how global and pointwise regularity are interconnected; wavelet analysis therefore is a natural tool in order to investigate this question and this explains why it was at the origin of major advances in multifractal analysis both in theory and applications.

We now recall the definition of orthonormal wavelet bases. For the sake of notational simplicity, we assume in all the remaining of Section 2 that $d = 1$, i.e. the functions we consider are defined on \mathbb{R} , extensions in several variables being straightforward. Let $\varphi(x)$ denote a smooth function with fast decay, and good joint time-frequency localization, referred to as the *scaling function*, and let $\psi(x)$ denote an oscillating function (with N first vanishing moments), with fast decay, and good joint time-frequency localization, referred to as the *wavelet*. These functions can be chosen such that the

$$\varphi(x - k), \quad \text{for, } k \in \mathbb{Z} \quad (22)$$

and

$$2^{j/2} \psi(2^j x - k), \quad \text{for, } j \geq 0, k \in \mathbb{Z} \quad (23)$$

form an orthonormal basis of $L^2(\mathbb{R})$ [97]. The wavelet coefficients of a function f are defined as

$$c_k = \int_{\mathbb{R}} f(x) \varphi(x - k) dx \quad \text{and} \quad c_{j,k} = 2^j \int_{\mathbb{R}} f(x) \psi(2^j x - k) dx \quad (24)$$

Note the use of an L^1 normalization for the wavelet coefficients that better fits local regularity analysis.

As stated above, the Hölder exponent can be used as a measurement of pointwise regularity in the locally bounded functions setting only, see [68]. Whether empirical data can be well-modelled by locally bounded functions or not can be determined numerically through the computation of the *uniform Hölder exponent* h_f^{min} , which, as for the scaling function, enjoys a function space characterization

$$h_f^{min} = \sup\{\alpha : f \in C^\alpha(\mathbb{R})\}, \quad (25)$$

where $C^\alpha(\mathbb{R})$ denotes the usual Hölder spaces. Assuming that φ and ψ are smooth enough and that ψ has enough vanishing moments, then the exponent h_f^{min} has the following simple wavelet characterization:

$$h_f^{min} = \liminf_{j \rightarrow +\infty} \frac{\log \left(\sup_k |c_{j,k}| \right)}{\log(2^{-j})}. \quad (26)$$

It follows that, if $h_f^{min} > 0$, then f is a continuous function, whereas, if $h_f^{min} < 0$, then f is not a locally bounded function, see [3, 69].

In numerous real world applications the restriction $h_f^{min} > 0$ constitutes a severe limitation; we will meet such examples in the case of physiological data (see also [3] for other examples). From a practical point of view, the regularity of the wavelets should be larger than h_f^{min} in order to compute the estimation of h_f^{min} . In the applications that we will see later, we took Daubechies compactly supported wavelets of increasing regularity and we stopped as soon as we found a threshold beyond which there is no more modification of the results. In our case, we stopped at order 3. In applications, the role of h_f^{min} is twofold: It can be used as a classification parameter and it tells whether a multifractal analysis based on the Hölder exponent is licit. Unlike other multifractality parameters that will be introduced

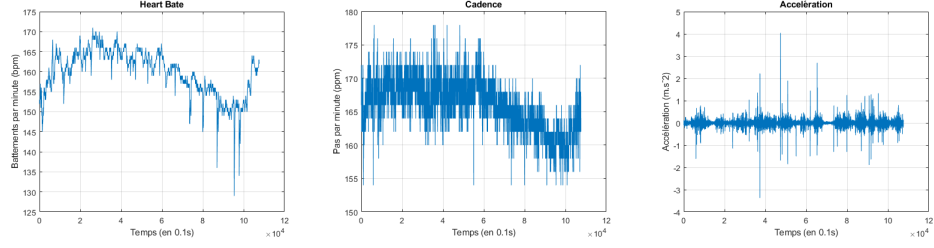


Figure 1: Representation of data: heart rate (left) in beats per minute, cadence (middle) in steps per minute and acceleration (top) in meters per second squared. The time scale is in 0.1s

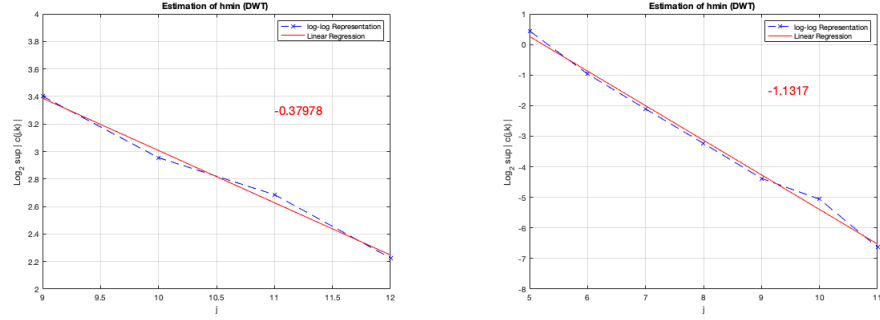


Figure 2: Estimation by log-log regression of the h_{min} of a heart rate (left) and an acceleration (right). The points of the regression line up successfully along a close to straight line thus showing that the values of h_{min} , are precisely estimated and are negative. It follows that a multifractal analysis based on Hölder exponent cannot be performed on these data.

in the following, its computation does not require a priori assumptions: It can be defined in the widest possible setting of tempered distributions.

We represent these two types of data on Fig. 2 for a marathon runner. The race is composed of several stages including a warm-up at the beginning, a recovery at the end of the marathon, and several moments of small breaks during the marathon. The signal was cleaned by removing the data that did not correspond to the actual race period (warm-ups, recoveries and breaks) and by making continuous connections to keep only the homogeneous parts. This type of connection is suitable for regularities exponents lower than 1 as in the case of our applications.

If $h_f^{min} < 0$, then a multifractal analysis based on the Hölder exponent cannot be developed, and the question whether a multifractal analysis based on the p -exponent can be raised. Wavelet coefficients can also be used to determine whether f locally belongs to L^p or not (which is the a priori requirement needed in order to use the corresponding p -exponent), see [69, 2, 3]: Indeed, a simple wavelet criterium can be applied to check this assumption,

through the computation of the *wavelet structure function*. Let

$$S_c(j, p) = 2^{-j} \sum_k |c_{j,k}|^p. \quad (27)$$

The *wavelet scaling function* is defined as

$$\forall p > 0, \quad \eta_f(p) = \liminf_{j \rightarrow +\infty} \frac{\log(S_c(j, p))}{\log(2^{-j})}; \quad (28)$$

one can show that it coincides with the Kolmogorov scaling function if $p > 1$, see [57]. The following simple criterion can be applied in order to check if data locally belong to L^p [74]:

$$\left. \begin{array}{ll} \text{if } \eta_f(p) > 0 & \text{then } f \in L_{loc}^p, \\ \text{if } \eta_f(p) < 0 & \text{then } f \notin L_{loc}^p. \end{array} \right\} \quad (29)$$

Remarks: The wavelet scaling function enjoys the same property as h_f^{min} : Its computation does not require some a priori assumptions on the data, and it can be defined in the general setting of tempered distributions. Note that it is also defined for $p \in (0, 1]$; in that case the Sobolev space interpretation of the scaling function has to be slightly modified: In Def. 1 the Lebesgue space L^p has to be replaced by the real Hardy spaces H^p , see [97] for the notion of Hardy spaces and their wavelet characterization. Note that these function space interpretations imply that the wavelet scaling function does not depend on the specific (smooth enough) wavelet basis which is used; it also implies that it is unaltered by the addition of a smooth function, or by a smooth change of variables, see [2] and ref. therein. For the same reasons, these properties also hold for the exponent h_f^{min} ; they are required in order to derive intrinsic parameters for signal or image classification. In the following, we shall refer to them as *robustness properties*. In applications (28) can be used only if $\eta_f(p)$ can be determined by a log-log plot regression, i.e. when the limit actually is a limit, see e.g. Fig. 4. This means that the structure functions (27) satisfy $S_c(j, p) \sim 2^{-\eta_f(p)j}$ in the limit of small scales, a phenomenon coined *scale invariance*. The practical relevance of the wavelet scaling function (and other multifractal parameters that we will meet later), comes from the fact that it can be used for classification of signals and images without assuming that the data follow an a priori model.

2.5 Wavelet pointwise regularity characterizations

One advantage of orthonormal wavelet based methods is that they allow to construct a multifractal analysis which is tailored for a given p -exponent, which is not the case of the alternative methods we mentioned. We shall see in Sections 2.6 and 2.9 the benefits of this extra flexibility. For this purpose, we have to construct multiresolution quantities (i.e., in this context, a non-negative function defined on the collection of dyadic cubes) which are fitted to p -exponents. We start by introducing more adapted notations for wavelets and wavelet coefficients; instead of the two indices (j, k) , we will use dyadic intervals (14) and,

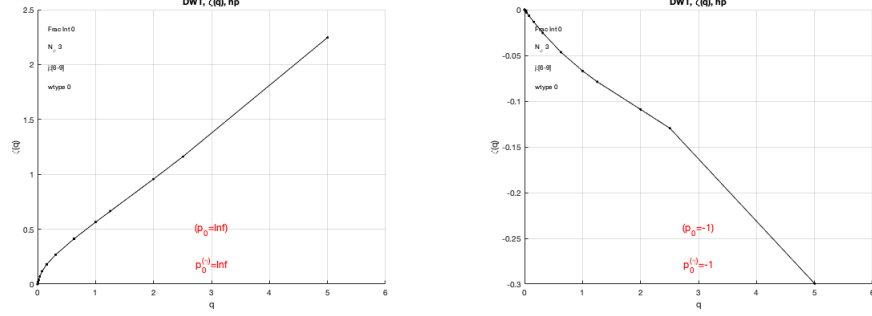


Figure 3: Wavelet scaling function of heart rate (left) and cadence (right) of a marathon runner. It allows to determine the values of p such that $\eta_f(p) > 0$. We conclude that a multifractal analysis based on p -exponents is directly possible for heart rate data, but not for the cadence, where the analysis will have to be carried out on a fractional integral of the data

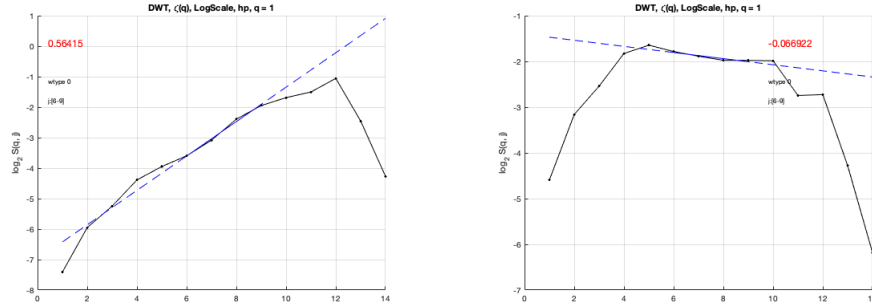


Figure 4: Estimation by log-log regression of the wavelet scaling function of heart rate (left) and cadence (right) for $p = 1$. The slope of the regression is positive for heart rate and negative for cadence. These regressions, estimated for a sufficiently large number of values of p allow to plot the wavelet scaling functions, as shown in Fig. 3

accordingly, $c_\lambda = c_{j,k}$, and $\psi_\lambda = \psi_{j,k}$. The wavelet characterization of p -exponents requires the definition of p -leaders. If $f \in L^p_{loc}(\mathbb{R})$, the wavelet p -leaders of f are defined as

$$\ell_{j,k}^{(p)} \equiv \ell_\lambda^{(p)} = \left(\sum_{\lambda' \subset 3\lambda} |c_{\lambda'}|^p 2^{j-j'} \right)^{1/p}, \quad (30)$$

where $j' \geq j$ is the scale associated with the sub-cube λ' included in 3λ (i.e. λ' has width $2^{-j'}$). Note that, when $p = +\infty$ (and thus $f \in L^\infty_{loc}(\mathbb{R})$), p -leaders boil down to *wavelet leaders*

$$\ell_\lambda = \sup_{\lambda' \subset 3\lambda} |c_{\lambda'}|,$$

[63, 113].

Let us indicate where such quantities come from. They are motivated by constructing quantities based on simple conditions on wavelet coefficients and which well approximate the local L^p norm of Definition 5. For that purpose we use the wavelet characterization of the Besov space $B_p^{0,p}$ which is “close” to L^p (indeed the classical embeddings between Besov and L^p spaces imply that $B_p^{0,1} \hookrightarrow L^p \hookrightarrow B_p^{0,\infty}$); with the normalization we chose for wavelet coefficients, the wavelet characterization of $B_p^{0,p}$ is given by

$$f \in B_p^{0,p} \quad \text{if} \quad \sum_k |c_k|^p < \infty \quad \text{and} \quad \sum_{j,k} 2^{(sp-1)j} |c_{j,k}|^p < \infty,$$

see [97] and, because of the localization of the wavelets, the restriction of the second sum to the dyadic cubes $\lambda' \subset 3\lambda$ yields an approximation of the local L^p norm of $f - P$ around the interval λ (the subtraction of the polynomial P comes from the fact that the wavelets have vanishing moments so that P is reconstructed by the first sum in (22), and the wavelet coefficients $c_{j,k}$ of f and $f - P$ coincide). Actually, the uniform regularity assumption $\eta_f(p) > 0$ (which we will make) implies that the quantities (30) are finite.

Denote by $\lambda_{j,k}(x)$ the unique dyadic interval of length 2^{-j} which includes x ; a key result is that both the Hölder exponent and the p -exponent can be recovered from, respectively, wavelet leaders and p -leaders, according to the following formula.

Definition 6 *Let $h(x)$ be a pointwise exponent and (d_λ) a multiresolution quantity indexed by the dyadic cubes. The exponent h is derived from the (d_λ) if*

$$\forall x, \quad h(x) = \liminf_{j \rightarrow +\infty} \frac{\log(d_{\lambda_{j,k}(x)})}{\log(2^{-j})}. \quad (31)$$

It is proved in [66, 69, 73] that if $\eta_f(p) > 0$, then the p -exponent is derived from p -leaders, and, if $h_f^{min} > 0$, then the Hölder exponent is derived from wavelet leaders. Note that the notion of p -exponent can be extended to values of p smaller than 1, see [65]; this extension requires the use of “good” substitutes of the L^p spaces for $p < 1$ which are supplied by the real Hardy spaces H^p . The important practical result is that the p -leaders associated with this notion also are given by (30).

In applications, one first computes the exponent h_f^{min} and the function $\eta_f(p)$. If $h_f^{min} > 0$, then one has the choice of using either p -leaders or wavelet leaders as multiresolution quantities. Though leaders are often preferred because of the simple interpretation that they yield in terms of the most commonly used (Hölder) exponent, it has been remarked that p -leaders constitute a quantity which displays better statistical properties, because it is based on averages of wavelet coefficients, instead of a supremum, i.e. a unique extremal value, see [4] and ref. therein. If both $h_f^{min} < 0$ and $\eta_f(p) < 0$ for all ps , then one cannot use directly these techniques and one performs a (fractional) integration on the data first. If one wants to use wavelet leaders, the order of integration s has to satisfy $s > -h_f^{min}$ since $h_{f(-s)}^{min} = h_f^{min} + s$. Similarly, in the case of p -leaders it follows immediately from the Sobolev interpretation (7) of the wavelet scaling function that

$$\eta_{f(-s)}(p) = ps + \eta_f(p).$$

Thus, if $\eta_f(p) < 0$, then an analysis based on p -leaders will be valid if the order of fractional integration s applied to f satisfies $s > -\eta_f(p)/p$. In practice, one does not perform a fractional integration on the data, but one simply replaces the wavelet coefficients $c_{j,k}$ by $2^{-sj}c_{j,k}$, which leads to the same scaling functions [3], and has the advantage of being performed at no extra computational cost.

2.6 Towards a classification of pointwise singularities

In Section 2.3 we motivated the introduction of alternative pointwise regularity exponents by the requirement of having a tool available for non locally bounded functions, which allows to deal directly with the data without having recourse to a smoothing procedure first; but this variety of exponents can also serve another purpose: By comparing them, one can draw differences between several types of singularities. This answers an important challenge in several areas of science; for example, in fully developed turbulence, some models predict the existence of extremely oscillating structures such as (2) and the key signal processing problem for the detection of gravitational waves also involves the detection of pointwise singularities similar to (2) in extremely noisy data [47].

Let us start with a simple example: Among the functions which satisfy $h_f(x_0) = \alpha$, the most simple pointwise singularities are supplied by *cusps* singularities, i.e. by functions which “behave” like

$$\mathcal{C}_\alpha(x) = |x - x_0|^\alpha \quad (\text{if } \alpha > 0 \text{ and } \alpha \notin 2\mathbb{N}). \quad (32)$$

How can we “model” such a behavior? A simple answer consists in remarking that the primitive of (32) is of the same form, and so on if we iterate integrations. Since the mapping $t \rightarrow h_{f(-t)}(0)$ is concave [9], it follows that (32) satisfies

$$\forall t > 0, \quad h_{\mathcal{C}_\alpha(-t)}(t_0) = \alpha + t.$$

For cusp singularities, the pointwise Hölder exponent is exactly shifted by the order of integration. This is in sharp contrast with the chirps (2), for which a simple integration by

parts yields that the Hölder exponent of its n -th iterated primitive is

$$\forall n \in \mathbb{N}, \quad h_{\mathcal{O}_{\alpha,\beta}^{(-n)}}(t_0) = \alpha + (1 + \beta)n,$$

from which it easily follows that the fractional primitives of the chirp satisfy

$$\forall t > 0, \quad h_{\mathcal{O}_{\alpha,\beta}^{(-t)}}(t_0) = \alpha + (1 + \beta)t,$$

[9]. We conclude from these two typical examples that inspecting simultaneously the Hölder exponents of f and its primitives, or its fractional integrals, allows to put in light that oscillating behaviour of f in the neighbourhood of its singularities which is typical of (2) (see [107] for an in-depth study of the information revealed by the mapping $t \rightarrow h_{f^{(-t)}}(t_0)$). To that end, the following definition was proposed, which encapsulates the relevant “oscillatory” information contained in this function, using a single parameter.

Definition 7 *Let $f : \mathbb{R}^d \rightarrow \mathbb{R}$ be such that $f \in L_{loc}^p$. If $h_f^p(x_0) \neq +\infty$, then the oscillation exponent of f at x_0 is*

$$\mathcal{O}_f(x_0) = \left(\frac{\partial}{\partial t} h_{f^{(-t)}}^p(x_0) \right)_{t=0^+} - 1. \quad (33)$$

Remark: In theory, a dependency in p should appear in the notation since f belongs to several L^p spaces. However, in practice, a given p is fixed, and this inaccuracy does not pose problems.

The choice of taking the derivative at $t = 0^+$ is motivated by a robustness argument: The exponent should not be perturbed when adding to f a smoother term, i.e. a term that would be a $O(|x - x_0|^h)$ for an $h > h_f(x_0)$; it is a consequence of the following lemma, which we state in the setting of Hölder exponents (i.e. we take $p = +\infty$ in Definition 7).

Lemma 1 *Let f be such that $h_f(x_0) < +\infty$ and $\mathcal{O}_f(x_0) < +\infty$; let $g \in C^\alpha(x_0)$ for an $\alpha > h_f(x_0)$. Then, for s small enough, the Hölder exponents of $(f + g)^{(-s)}$ and of $f^{(-s)}$ coincide.*

Proof: By the concavity of the mapping $s \rightarrow h_{f^{(-s)}}(x_0)$, see [67, 6], it follows that

$$h_{f^{(-s)}}(x_0) \leq h_f(x_0) + (1 + \mathcal{O}_f(x_0))s;$$

but one also has $h_{g^{(-s)}}(x_0) \leq \alpha + s$; so that, for s small enough, $h_{g^{(-s)}}(x_0) > h_{f^{(-s)}}(x_0)$, and it follows that $h_{(f+g)^{(-s)}}(x_0) = h_{f^{(-s)}}(x_0)$.

The oscillation exponent takes the value β for a chirp; it is the first of *second generation exponents* that do not measure a regularity, but yield additional information, paving the way to a richer description of singularities. In order to go further in this direction, we consider another example: *Lacunary combs*, which were first considered in [67, 6] (we actually deal here with a slight variant). Let $\phi = \mathbb{1}_{[0,1]}$.

Definition 8 Let $\alpha \in \mathbb{R}$ and $\gamma > \omega > 0$. The lacunary comb $F_{\omega,\gamma}^\alpha$, is

$$F_{\omega,\gamma}^\alpha(x) = \sum_{j=1}^{\infty} 2^{-\alpha j} \phi(2^{\gamma j}(x - 2^{-\omega j})). \quad (34)$$

We consider its behaviour near the singularity at $x_0 = 0$: if $\alpha > -\gamma$, then $F_{\omega,\gamma}^\alpha \in L^1(\mathbb{R})$ and it is locally bounded if and only if $\alpha \geq 0$. In that case, one easily checks that

$$h_{F_{\omega,\gamma}^\alpha}(0) = \frac{\alpha}{\omega}, \quad \text{and} \quad h_{F_{\omega,\gamma}^{\alpha,(-1)}}(0) = \frac{\alpha + \gamma}{\omega} \quad (35)$$

and one obtains (see [6]) that $\mathcal{O}_{F_{\omega,\gamma}^\alpha}(0) = \frac{\gamma}{\omega} - 1$.

We conclude that chirps and lacunary combs are two examples of oscillating singularities. They are, however, of different nature: In the second case, oscillation is due to the fact that this function vanishes on larger and larger proportions of small balls centered at the origin (this is detailed in [67], where this phenomenon is precisely quantified through the use of *accessibility exponent* of a set at a point). On the other hand, chirps are oscillating singularities for a different reason: It is due to very fast oscillations, and compensations of signs. This can be checked by verifying that the oscillation exponent of $|\mathcal{C}_{\alpha,\beta}|$ at 0 vanishes.

We will now see that this difference can be put in evidence by considering the variations of the p -exponent. Comparing the p -exponents of chirps and lacunary combs allows to draw a distinction between their singularities; indeed, for $p \geq 1$, see [74],

$$h_{F_{\omega,\gamma}^\alpha}^p(0) = \alpha + \frac{1}{p} \left(\frac{\gamma}{\omega} - 1 \right) \quad (36)$$

whereas a straightforward computation yields that

$$\forall p, \quad h_{\mathcal{C}_{\alpha,\beta}}^p(0) = \alpha.$$

We conclude that the p -exponent of $F_{\omega,\gamma}^\alpha$ varies with p , whereas the one of $\mathcal{C}_{\alpha,\beta}$ does not. We will introduce another pointwise exponent which captures the lacunarity of the combs; it requires first the following notion: If $f \in L_{loc}^p$ in a neighborhood of x_0 for $p > 1$, the *critical Lebesgue index* of f at x_0 is

$$p_f(x_0) = \sup\{p : f \in L_{loc}^p(\mathbb{R}) \text{ in a neighborhood of } x_0\}. \quad (37)$$

The p -exponent at x_0 is defined on the interval $[1, p_f(x_0)]$ or $[1, p_f(x_0))$. We denote: $q_f(x_0) = 1/p_f(x_0)$. Note that $p_f(x_0)$ can take the value $+\infty$. An additional pointwise exponent, which, in the case of lacunary combs, quantifies the sparsity of the “teeth” of the comb, can be defined as follows see [67]. Its advantage is that it quantifies the “lacunarity information” using a single parameter instead of the whole function $p \rightarrow h_f^{(p)}(x_0)$.

Definition 9 Let $f \in L_{loc}^p$ in a neighborhood of x_0 for a $p > 1$. The *lacunarity exponent* of f at x_0 is

$$L_f(x_0) = \frac{\partial}{\partial q} \left(h_f^{(1/q)}(x_0) \right)_{q=q_f(x_0)^+}. \quad (38)$$

This quantity may have to be understood as a limit when $q \rightarrow q_f(x_0)$, since $h_f^{1/q}(x_0)$ is not necessarily defined for $q = q_f(x_0)$. This limit always exists as a consequence of the concavity of the mapping $q \rightarrow h_f^{1/q}(x_0)$, and it is nonnegative (because this mapping is increasing).

The lacunarity exponent of $F_{\omega,\gamma}^\alpha$ at 0 is $\frac{\gamma}{\omega} - 1$, which puts into light the fact that this exponent allows to measure how $F_{\omega,\gamma}^\alpha$ vanishes on "large sets" in the neighborhood of 0 (see [67] for a precise statement). Furthermore the oscillation exponent of $F_{\omega,\gamma}^\alpha$ at 0 is $\frac{\gamma}{\omega} - 1$, so that it coincides with the lacunarity exponent. The oscillation exponent is always larger than the lacunarity exponent. A way to distinguish between the effect due to lacunarity and the one due to cancellations is to introduce a third exponent, the *cancellation exponent*

$$\mathcal{C}_f(x_0) = \mathcal{O}_f(x_0) - L_f(x_0).$$

The lacunarity and the cancellation exponents lead to the following classification of pointwise singularities see [6].

Definition 10 *Let f be a tempered distribution on \mathbb{R} :*

- f has a **canonical singularity** at x_0 if $\mathcal{O}_f(x_0) = 0$.
- f has a **balanced singularity** at x_0 if $L_f(x_0) = 0$ and $\mathcal{C}_f(x_0) \neq 0$.
- f has a **lacunary singularity** at x_0 if $\mathcal{C}_f(x_0) = 0$ and $L_f(x_0) \neq 0$.

Cusps are typical examples of canonical singularities, chirps are typical examples of balanced singularities and lacunary combs are typical examples of lacunary singularities.

Many probabilistic models display lacunary singularities: It is the case e.g. for random wavelet series [67, 6], some Lévy processes, see [19] or fractal sums of pulses [104]. Note that our comprehension of this phenomenon is very partial: For instance, in the case of Lévy processes, the precise determination of the conditions that a Lévy measure should satisfy in order to guarantee the existence of lacunary singularities has not been worked out: in [19], P. Balanca proved that some self-similar Lévy processes with even Lévy measure display oscillating singularities, which actually turn out to be lacunary singularities and also that Lévy processes which have only positive jumps do not display such singularities; and, even in these cases, only a lower bound on their Hausdorff dimensions has been obtained. In other words, for Lévy processes, a joint multifractal analysis of the Hölder and the lacunarity exponent remains to be worked out. Note also that there exists much less examples of functions with balanced singularities: In a deterministic setting it is the case for the Riemann function [75] at certain rational points. However, to our knowledge, stochastic processes with balanced singularities have not been met up to now.

Another important question is to find numerically robust ways to determine if a signal has points where it displays balanced or lacunary singularities. This question is important in several areas of physics; for instance, in hydrodynamic turbulence, proving the presence of oscillating singularities would validate certain vortex stretching mechanisms which have been proposed, see [51]. Another motivation is methodological: if a signal only has canonical

singularities, then its p -multifractal spectrum does not depend on p and its singularity spectrum is translated by t after a fractional integral of order, so that all methods that can be used to estimate its multifractal spectrum yield the same result (up to a known shift in the case of a fractional integration). An important questions related with the multifractal formalism is to determine if some of its variants allow to throw some light on these problems. Motivated by applications to physiological data, we shall come back to this question in Sections 2.9 and 3.3.

Note that the choice of three exponents to characterize the “behaviour” of a function in the neighbourhood of one of its singularities may seem arbitrary; indeed, one could use the very complete information supplied by the following two variables function: If f is a tempered distribution, then the *fractional exponent* of f at x_0 is the two variable function

$$\mathcal{H}_{f,x_0}(q, t) = h_{f(-t)}^{1/q}(x_0) - t,$$

see [6] where this notion is introduced and its properties are investigated. However, storing the pointwise regularity behaviour through the use of a two-variables function defined at every point is unrealistic, hence the choice to store only the information supplied by the three parameters we described. This choice is motivated by two conflicting requirements: On one hand, one wishes to introduce mathematical tools which are sophisticated enough to describe several “natural” behaviours that can show up in the data, such as those supplied by cusps, chirps, and lacunary combs. On other hand, at the end, classification has to bear on as little parameters as possible in order to be of practical use in applications; the goal here is to introduce a multivariate multifractal analysis based on a single function f , but applied to several pointwise exponents associated with f (say two or three among a regularity, a lacunarity and a cancellation exponent).

Our theoretical comprehension of which functions can be pointwise exponents is extremely partial, see [106] for a survey on this topic: It has been known for a long time that a pointwise Hölder exponent $h_f(x)$ can be any nonnegative function of x which can be written as a liminf of a sequence of continuous functions, see [55, 16, 41], but the same question for p -exponents is open (at least in the case where it takes negative values). Similarly, which couples of functions $(h(x), O(x))$ can be the joint Hölder and oscillation exponents of a function also is an open question (see [59] for partial results), and it is the same if we just consider the oscillation exponent, or couples including the lacunarity exponent. One meets similar limitations for multifractal spectra: In the univariate setting supplied by the multifractal Hölder spectrum, the general form of functions which can be multifractal spectra is still open; nonetheless a partial result is available: functions which can be written as infima of a sequence of continuous functions are multifractal spectra [54]; additionally, as soon as two exponents are involved, extremely few results are available. For instance, if f is a locally bounded function, define its *bivariate oscillation spectrum* as

$$\mathcal{D}_f(H, \beta) = \dim\{h : h_f(x) = H \quad \text{and} \quad \mathcal{O}_f(x) = \beta\}.$$

Which functions of two variables $D(H, \beta)$ can be bivariate oscillation spectra is a completely open problem.

2.7 Mathematical results concerning the multifractal formalism

We now consider a general setting where $h : \mathbb{R} \rightarrow \mathbb{R}$ is a pointwise exponent derived from a multiresolution quantity $d_\lambda (= d_{j,k})$ according to Def. 6, and defined in space dimension d . The associated multifractal spectrum \mathcal{D} is

$$\mathcal{D}(H) = \dim(\{x : h(x) = H\}).$$

The *support* of the spectrum is the image of the mapping $x \rightarrow h(x)$, i.e. the collection of values of H such that

$$\{x \in \mathbb{R} : h(x) = H\} \neq \emptyset$$

(note that this denomination, though commonly used, is misleading, since it may not coincide with the mathematical notion of support of a function).

The *leader scaling function* associated with the multiresolution quantities $(d_{j,k})$ is

$$\forall q \in \mathbb{R}, \quad \zeta_f(q) = \liminf_{j \rightarrow +\infty} \frac{\log \left(2^{-j} \sum_k |d_{j,k}|^q \right)}{\log(2^{-j})}. \quad (39)$$

Note that, in contradistinction with the wavelet scaling function, it is also defined for $p < 0$. Referring to “leaders” in the name of the scaling function does not mean that the $d_{j,k}$ are necessarily obtained as wavelet leaders or wavelet p -leaders, but only to prevent any confusion with the wavelet scaling function. The *Legendre spectrum* is

$$\mathcal{L}(H) := \inf_{q \in \mathbb{R}} (1 + qH - \zeta_f(q)). \quad (40)$$

As soon as relationships such as (31) hold, then the following upper bound is valid

$$\forall H, \quad \mathcal{D}(H) \leq \mathcal{L}(H) \quad (41)$$

(see [63] for particular occurrences of this statement, and [2] for the general setting). However, for a number of synthetic processes with known $\mathcal{D}(H)$ (and for a proper choice of the multiresolution quantity), this inequality turns out to be an equality, in which case, we will say that the *multifractal formalism holds*. The leader scaling functions obtained using wavelet leaders or p -leaders can be shown to enjoy the same robustness properties as listed at the end of Section 2.4, see [2] (it is therefore also the case for the Legendre spectrum). It follows from their mathematical and numerical properties that wavelet leader based techniques form the state of the art for real-life signals multifractal analysis.

In applications, one cannot have access to the regularity exponent at every point in a numerically stable way, and thus $\mathcal{D}(H)$ is inaccessible; this explains why, in practice, $\mathcal{L}(H)$ is the only computationally available spectrum, and it is used as such in applications. However, information on the pointwise exponent may be inferred from the Legendre spectrum. Such results are collected in the following theorem, where they are stated in decreasing order of generality.

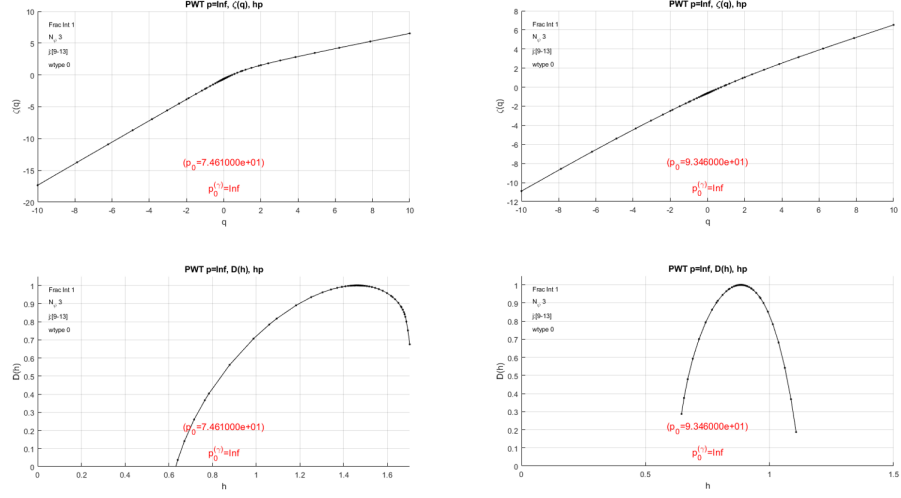


Figure 5: Representation of scale function and the univariate Hölder Legendre spectra of the primitives of heart beat frequency (left) and cadence (right) of one marathon runner during the entire race. the multiresolution quantities used in these derivation are the wavelet leaders of the primitive of the data

Theorem 1 *Let $h : \mathbb{R} \rightarrow \mathbb{R}$ be a pointwise exponent, and assume that it is derived from multiresolution quantities $d_{j,k}$ according to Def. 6. The following results on h hold:*

- *Let*

$$h^{\min} = \liminf_{j \rightarrow +\infty} \frac{\log \left(\sup_k d_{j,k} \right)}{\log(2^{-j})} \quad \text{and} \quad h^{\max} = \liminf_{j \rightarrow +\infty} \frac{\log \left(\inf_k d_{j,k} \right)}{\log(2^{-j})} \quad (42)$$

then

$$\forall x \in \mathbb{R} \quad h^{\min} \leq h(x) \leq h^{\max}. \quad (43)$$

- *If the Legendre spectrum has a unique maximum for $H = c_1$, then*

$$\text{for almost every } x, \quad h(x) = c_1; \quad (44)$$

- *If the leader scaling function (39) associated with the $d_{j,k}$ is affine, then f is a monohölder function, i.e.*

$$\exists H_0 : \quad \forall x, \quad h(x) = H_0,$$

where H_0 is the slope of the leader scaling function.

Remark: The last statement asserts that, if h is a pointwise exponent associated with a function f , then f is a monohölder function. This result has important implications in modeling since it yields a numerically simple test, based on global quantities associated with the signal, and which yields the pointwise exponent everywhere. This is in strong

contradistinction with the standard pointwise regularity estimators, see e.g. [20] and ref. therein, which are based on local estimates, and therefore on few data thus showing strong statistical variabilities, and additionally often assume that the data follow some a priori models.

Proof: We first prove the upper bound in (43). Let $\alpha > h^{max}$; there exists a sequence $j_n \rightarrow +\infty$ such that

$$\log \left(\inf_k d_{j_n, k} \right) \geq \log(2^{-\alpha j_n}),$$

so that at the scales j_n all d_λ are larger than $2^{-\alpha j_n}$. It follows from (31) that

$$\forall x, \quad h(x) \leq \alpha,$$

and the upper bound follows. The proof of the lower bound is similar (see e. g. [70]).

The second statement is direct consequence of the following upper bounds for the dimensions of the sets

$$E_H^+ = \{h(x) \geq H\} \quad \text{and} \quad E_H^- = \{h(x) \leq H\} \quad (45)$$

which are a slight improvement of (41), see [70]:

Proposition 2 *Let h be a pointwise exponent derived from the multiresolution quantity $(d_{j,k})$. Then the following bounds hold:*

$$\dim(E_H^-) \leq \inf_{q>0} (1 + qH - \zeta_f(q)) \quad \text{and} \quad \dim(E_H^+) \leq \inf_{q<0} (1 + qH - \zeta_f(q)) \quad (46)$$

Let us check how (44) follows from this result. Note that the first (partial) Legendre transform yields the increasing part of $\mathcal{L}(H)$ for $H \leq c_1$ and the second one yields the decreasing part for $H \geq c_1$. If \mathcal{L} has a unique maximum for $H = c_1$, it follows from (46) that

$$\forall n, \quad \dim(E_{c_1-1/n}^-) < 1 \quad \text{and} \quad \dim(E_{c_1+1/n}^-) < 1.$$

All of these sets therefore have a vanishing Lebesgue measure, which is also the case of their union. But this union is $\{x : h(x) \neq c_1\}$. It follows that almost every x satisfies $h(x) = c_1$.

Finally, if the leader scaling function is affine, then its Legendre transform is supported by a point H_0 and takes the value $-\infty$ elsewhere. The upper bound (41) implies that, if $H \neq H_0$ the corresponding isoregularity set is empty. In other words, H_0 is the only value taken by the pointwise exponent, and f is a monohölder function.

Remarks:

If $h^{min} = h^{max}$, the conclusion of the first and last statement are the same. However, one can check that the condition $h^{min} = h^{max}$ is slightly less restrictive than requiring the leader scaling function to be affine (the two conditions are equivalent if, additionally, the \liminf in (42) is a limit).

The parameter c_1 defined in Theorem 1 can be directly estimated using log-log plot (see [3] and ref. therein), and, in practice it plays an important role in classification as we will see in the next section. When the multiresolution quantity used is the p -leaders of a function f , the associated exponent c_1 may depend on p , and we will mention this dependency and denote this parameter by $c_1(p, f)$. This is in contradistinction with the exponent h^{min} defined by (42), which, in the case of functions with some uniform Hölder regularity, coincides with the exponent h_f^{min} defined by (26) for leaders and p -leaders, as shown by the following lemma; note that it is actually preferable to compute it using (26), which has the advantages of being well defined without any a priori assumption on f .

Lemma 2 *Let $f : \mathbb{R} \rightarrow \mathbb{R}$ be such that $h_f^{min} > 0$. Then the h^{min} parameter computed using p -leaders all coincide with the h_f^{min} computed using wavelet coefficients.*

Let us sketch the proof of this result. Suppose that $h_f^{min} > 0$ and let $\alpha > 0$ be such that $\alpha < h_f^{min}$. Then, the wavelet coefficients of f satisfy

$$\exists C, \quad \forall j, k \quad |c_{j,k}| \leq C 2^{-\alpha j}.$$

Therefore the p -leaders of f satisfy

$$\begin{aligned} \ell_\lambda^{(p)} &\leq \left(\sum_{\lambda' \subset 3\lambda} (2^{-\alpha j'})^p 2^{j-j'} \right)^{1/p} \\ &\leq \left(\sum_{j' \geq j} 2^{-\alpha p j'} 2^{j-j'} \right)^{1/p} \leq C 2^{-\alpha j}; \end{aligned}$$

it follows that the corresponding p -leader is smaller than $|c_{\lambda_n}|$ so that the h^{min} computed using p -leaders is smaller than the one computed using wavelet coefficients. Conversely, by definition of h_f^{min} , there exists a sequence of dyadic intervals c_{λ_n} of width decreasing to 0, and such that

$$|c_{\lambda_n}| \sim 2^{-h_f^{min} j_n},$$

and the corresponding p -leader is larger than $|c_{\lambda_n}|$ so that the h^{min} computed using p -leaders is smaller than the one computed using wavelet coefficients.

The following result yields an important a priori bound on the dimensions of the singularity sets corresponding to negative regularity exponents, see [74].

Proposition 3 *Let $p > 0$, and let $f : \mathbb{R} \rightarrow \mathbb{R}$ be a function such that $\eta_f(p) > 0$. Then its p -spectrum satisfies*

$$\forall h, \quad \mathcal{D}_p(H) \leq 1 + Hp$$

Let us elaborate on the information supplied by the exponent $c_1(p, f)$: A direct consequence of (44) is that, if a signal f satisfies that the exponent $c_1(p, f)$ takes the same value for $p_1 < p_2$, then this implies that the p -exponent satisfies that

$$\text{for almost every } x, \quad h_f^{p_1}(x) = h_f^{p_2}(x),$$

which implies that the mapping $p \rightarrow h_f^{p_1}(x)$ is constant for $p \in [p_1, p_2]$; but, since the mapping $p \rightarrow h_f^{1/p}(x_0)$ is concave and increasing, see [67, 6], it follows that this mapping is constant for p small enough; as a consequence, the lacunarity exponent vanishes at x . Similarly, if, for a given p , $c_1(p, f^{(-1)}) - c_1(p, f) = 1$, this implies that

$$\text{for almost every } x, \quad h_{f^{(-1)}}^p(x) = h_f^p(x) + 1,$$

and the same argument as above, see [67, 6], yields the absence of oscillating singularities for almost every point. In other words, the computation of $c_1(p)$ yields a key information on the nature of the singularities a.e. of the signal, which we summarize in the following statement, which will have implications in the next section for the analysis of marathon runners data.

Proposition 4 *Let $f : \mathbb{R} \rightarrow \mathbb{R}$ be a function in L^p .*

If

$$\exists q > p : \quad c_1(p, f) = c_1(q, f),$$

then for almost every x , f has no lacunary singularity at x .

If f satisfies

$$\exists p : \quad c_1(p, f^{(-1)}) - c_1(p, f) = 1,$$

then, for almost every x , f has a canonical singularity at x .

These two results are characteristic of signals that only contain canonical singularities, see Section 2.6, and they also demonstrate that $c_1(p, f)$, which, in general, depends on the value of p is intrinsic for such data (see a contrario [67] where the exponent $c_1(p, f)$ of lacunary wavelet series is shown to depend on the value of p , and [104] where the same result is shown for random sums of pulses). Note that such results are available in the discrete wavelet approach only; they would not be possible using the WTMM or the MFDFA approaches, which do not allow to draw differences between various pointwise regularity exponents and therefore do not yield spectra fitted to different values of the p -exponent. To summarize, the advantages of the p -leader based multifractal analysis framework are: the capability to estimate negative regularity exponents, better estimation performances, and a refined characterization of the nature of pointwise regularities.

One important argument in favor of multifractal analysis is that it supplies robust classification parameters, in contradistinction with pointwise regularity which can be extremely erratic. Consider for instance the example of a sample path of a Lévy process without Brownian component (we choose this example because such processes now play a key role in statistical modeling): Its Hölder exponent is a random, everywhere discontinuous, function which cannot be numerically estimated or even drawn [58]: In any arbitrary small

interval $[a, b]$ it takes all possible values $H \in [0, H^{max}]$. On the opposite, the multifractal spectrum (which coincides with the Legendre spectrum) is extremely simple and robust to estimate numerically: It is a deterministic linear function on the interval $[0, H^{max}]$ (with $D(H^{max}) = 1$). This example is by no means accidental: though one can simply construct stochastic processes with a random multifractal spectrum (consider for instance a Poisson process restricted to an interval of finite length), large classes of classical processes have simple deterministic multifractal spectra (and Legendre spectra), though no simple assumption which would guarantee this results is known. The determination of a kind of “0-1 law” for multifractal spectra, which would guarantee that, under fairly general assumptions, the spectrum almost surely is a deterministic function, is a completely open problem, and its resolution would greatly improve our understanding of the subject. Even in the case of Gaussian processes, though it is known that such processes can have a random Hölder exponent [15], the possibility of having a random multifractal spectrum still is a open issue.

2.8 Generic results

Let us come back to the problem raised in Section 2.1 of estimating the size of the Hölder singularity sets of increasing functions which led us to the key idea that the Hausdorff dimension is the natural way to estimate this size. One can wonder if the estimate (15) that we found for the multifractal spectrum is optimal. In 1999, Z. Buczolich and J. Nagy answered this question in a very strong way, showing that it is sharp for a *residual* set of continuous increasing functions, see [35]. What does this statement precisely mean? Let E be the set of continuous increasing functions $f : \mathbb{R} \rightarrow \mathbb{R}$, endowed with the natural distance supplied by the sup norm. Then equality in (15) holds (at least) on a residual set in the sense of Baire categories, i.e. on a countable intersection of open dense sets.

This first breakthrough opened the way to genericity results in multifractal analysis. They were the consequence of the important remark that scaling functions for $p > 0$ can be interpreted as stating that f belongs to an intersection of Sobolev spaces E_η (in the case of the Kolmogorov scaling function) or of a variant of these spaces, the *oscillation spaces* in the case of the leader scaling function [64]. One easily checks that E_η is a complete metric space, and the Baire property therefore is valid (i.e. a countable intersection of open dense sets is dense). The question formulated by Parisi and Frisch in [100], can be reformulated in this setting: If equality in (41) cannot hold for *every* function in E_η (since e.g. because it contains C^∞ functions), nonetheless it holds on a residual set [61]. This result found many extensions: The first one consists in replacing the genericity notion supplied by Baire’s theorem by the more natural notion supplied by *prevalence*, which is an extension, in infinite dimensional function spaces of the notion of “Lebesgue almost everywhere”, see [40, 17] for the definition of this notion and its main properties, and [50] for its use in the setting of multifractal analysis. The conclusions drawn in the Baire setting also hold in the prevalence setting, and raise the question of the determination of a stronger notion of genericity, which would imply both Baire and prevalence genericity, and which would be the “right” setting for the validity of the multifractal formalism. A natural candidate is supplied by the notion of *porosity*, see [116], but the very few results concerning multifractal analysis in this setting do not allow to answer this question yet. Note also that Baire and prevalence

results have been extended to the p -exponent setting [49], which allows to deal with spaces of functions that are not locally bounded. Another key problem concerning the generic validity of the multifractal formalism concerns the question of taking into account the information supplied by negative values of p in the scaling function (39). The main difficulty here is that the scaling function does not define a function space any longer, and the “right” notion of genericity which should be picked is completely open: Though Baire and prevalence do not really require the setting supplied by a (linear) function space, nonetheless these notions are not fitted to the setting supplied by a given scaling function which includes negative values of p . In [23] J. Barral and S. Seuret developed an alternative point of view which is less “data driven”: They reinterpreted the question in the following way: Given a certain scaling function $\eta(p)$, they considered the problem of constructing an ad hoc function space which is tailored so that generically (for the Baire setting), functions in such a space satisfy the multifractal formalism for the corresponding scaling function, including its values for $p < 0$ (and Legendre spectrum). Another limitation of the mathematical results of genericity at hand is that they are not able to take into account *selfsimilarity* information: In (28), in order to introduce a quantity which is always well-defined, and corresponds to a function space regularity index, the scaling function is defined by a \liminf . But, most of the time, what is actually observed on the data (and what is really needed in order to obtain a numerically robust estimate) is that this \liminf actually is a true limit, which means that the L^p averages of the data display exact power-law behaviours at small scales. Up to now, one has not been able to incorporate this type of information in the function space modeling developed.

2.9 Implications on the analysis of marathon runners data

The increasing popularity of marathons today among all ages and levels is inherited from the human capacity to run long distances using the aerobic metabolism [88], which led to a rising number of amateur marathon runners who end the 42,195 km between 2h40min and 4h40min. Therefore, even if nowadays, marathon running becomes “commonplace”, compared with ultra-distance races, this mythic Olympic race is considered to be the acme of duration and intensity [94]. Running a marathon remains scary and complex due to the famous “hitting the wall” phenomenon, which is the most iconic feature of the marathon [29]. This phenomenon was previously evaluated in a large-scale data analysis of late-race pacing collapse in the marathon [111]; [110] presented an analysis of 1.7 million recreational runners, focusing on pacing at the start and end of the marathon, two particularly important race stages. They showed how starting or finishing too quickly could result in poorer finish-times, because fast starts tend to be very fast, leading to endurance problems later, while fast finishes suggest overly cautious pacing earlier in the race [110]. Hence, the definition of a single marathon pace is based on the paradigm that a constant pace would be the ideal one. However, in [31], a 3 years study shows that large speed and pace variations are the best way to optimize performance. Marathon performance depends on pacing oscillations between non symmetric extreme values [102]. Heart rate (HR) monitoring, which reflects exercise intensity and environmental factors, is often used for running strategies in marathons. However, it is difficult to obtain appropriate feedback for only the HR value

since, as we saw above, the cardiovascular drift occurs during prolonged exercise. Therefore, now we have still to investigate whether this pace (speed) variation has a fractal behavior and if so, whether this is the case for the runners's heart rate which remains a pacer for the runners who aim to keep their heart rate in a submaximal zone (60-80 % of the maximal heart rate) [94]. Here, we hypothesized that marathonians acceleration (speed variation), cadence (number of steps per minute) and heart rate time series follow a multifractal formalism and could be described by a self similar functions. Starting in the 1990s, many authors demonstrated the fractal behavior of physiological data such as heart rate, arterial blood pressure, and breath frequency of human beings, see e.g. [5, 53]. In 2005, using the Wavelet Transform Maxima Method, E. Wesfreid, V. L. Billat and Y. Meyer [114] performed the first multifractal analysis of marathonians heartbeats. This study was complemented in 2009 using the DFA (Detrended Fluctuation Analysis) and wavelet leaders applied on a primitive of the signal [30]. Comparing the outputs of these analyses is hasardous; indeed, as already mentioned, these methods are not based on the same regularity exponents: WTMM is adapted to the *weak scaling exponent* [98], DFA to the p -exponent for $p = 2$ [74, 87], and wavelet leaders to the Hölder exponent [63]. In the following, we will propose a method of digital multifractal analysis of signals based on p -leaders, which, in some cases, can avoid performing fractional integrations (or primitives) and thus transform the signal. In [30], it was put in evidence that multifractal parameters associated with heart beat intervals evolve during the race when the runner starts to be deprived of glycogen (which is the major cause of the speed diminution at the end of the race. This study also revealed that fatigue decreases the running speed and affects the regularity properties of the signal which can be related with the feelings of the runner measured by the Rate of Perception of Exhaustion (RPE), according to the psychophysiological scale of Borg (mainly felt through the breathing frequency). In addition, there is a consistent decrease in the relationship between speed, step rate, cardiorespiratory responses (respiratory rate, heart rate, volume of oxygen consumed), and the level of Rate of Perception of Exhaustion (RPE), as measured by Borg's psychophysiological scale. The runner does not feel the drift of his heart rate, in contradistinction with his respiratory rate. These physiological data are not widely available and only heart rate and stride rate are the measures available to all runners for economic reasons. Moreover, these data are generated heartbeat by heartbeat and step by step.

Our purpose in this section is to complement these studies by showing that a direct analysis on the data is possible if using p -leaders (previous studies using the WTMM or the standard leaders had to be applied to a primitive of the signal), and that they lead to a sharper analysis of the physiological modifications during the race. We complement the previous analyses in order to demonstrate the modifications of multifractal parameters during the race, and put in evidence the physiological impact of the intense effort after the 20th Km. For that purpose, we will perform a multifractal analysis based on p -leaders.

We analyzed the heartbeat frequency of 8 marathon runners (men in the same age area). Fig.2 shows the determination of exponents h_f^{min} for heartbeat frequency and cadence through a log-log regression; the regression is always performed between the scales $j = 8$ and $j = 11$ (i.e. between 26s and 3mn 25s), which have been identified as the pertinent scales for such physiological data, see [5]. For most marathon runners, h_f^{min} is negative, see Table 1,

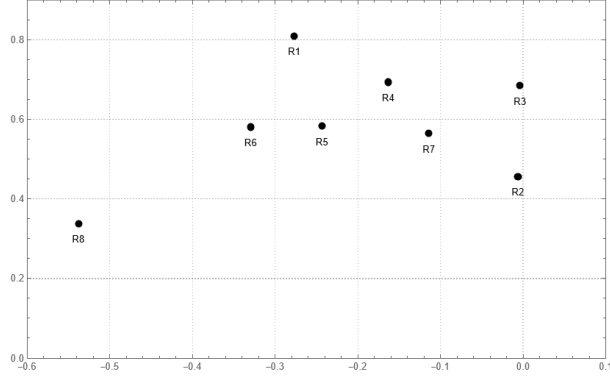


Figure 6: Representation of the pair $(H_{min}, c_1(p))$ with $p = 1$ deduced from the 1-spectrum of heart rate and computed for the entire race; H_{min} appears as the most relevant classification parameter. The isolated point on the left corresponds to R8, the most trained runner.

which justifies the use of p -leaders. We then compute the wavelet scaling function in order to determine a common value of p for which all runners satisfy $\eta(p) > 0$, see Fig. 3 where examples of wavelet scaling function are supplied for heartbeat frequency and cadence. In the case of heartbeat frequency, the computation of the 8 wavelet scaling functions yields that $p = 1$ and $p = 1.4$ can be picked. The corresponding p -leaders multifractal analysis is performed for these two values of p , leading to values of $c_1(p)$ which are also collected in Table 1.

Table 1: Multifractal Analysis of heartbeat frequency of marathon runners (Pr. : primitive)

	H_{min}	H_{min} of the Pr.	c_1 for $p = 1$	c_1 for $p = 1.4$	c_1 of the Pr. for $p = 1$	c_1 of the Pr. for $p = 1.4$
R1	-0,2768	0,7232	0,8099	0,8064	1,8242	1,8213
R2	-0,0063	0,9937	0,4564	0,4043	1,3926	1,3509
R3	-0,0039	0,9961	0,6856	0,6625	1,6942	1,6351
R4	-0,1633	0,8367	0,6938	0,6785	1,6653	1,6636
R5	-0,2434	0,7566	0,5835	0,5689	1,5401	1,5224
R6	-0,3296	0,6704	0,5809	0,5636	1,5644	1,5500
R7	0,1099	1,1099	0,5652	0,5483	1,4754	1,4379
R8	-0,5380	0,4620	0,3382	0,2977	1,2588	1,2086

In Fig. 6, the value of the couple $(h_f^{min}, c_1(p))$ is plotted (where we denote by $c_1(p)$ the value of H for which the maximum of the p -spectrum is reached). The values of $c_1(p)$ are very close to 0.4 whereas the values of h_f^{min} notably differ, and are clearly related with the level of practice of the runners. Thus M8 is the only trail runner and improved his personal record on that occasion; he practices more and developed a very uneven way of running. Table 1 shows that the values of $c_1(p)$ do not notably differ for different values of p and, when computed on a primitive of the signal, are shifted by 1. We are in the situation

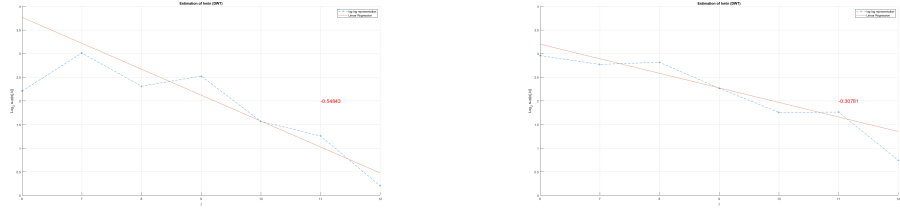


Figure 7: Estimation of h_f^{min} by log-log regression for the heart rate of a marathon runner at the beginning (50% first part of the race) on the left and the end (25% last part of the race) on the right. The clear difference of the values obtained shows that the exponent h_f^{min} is well fitted to characterize the evolution of physiological rythms during the race. These data, together with the evolution of the parameter $c_1(p)$, are collected in Fig.8 with $p = 1$.

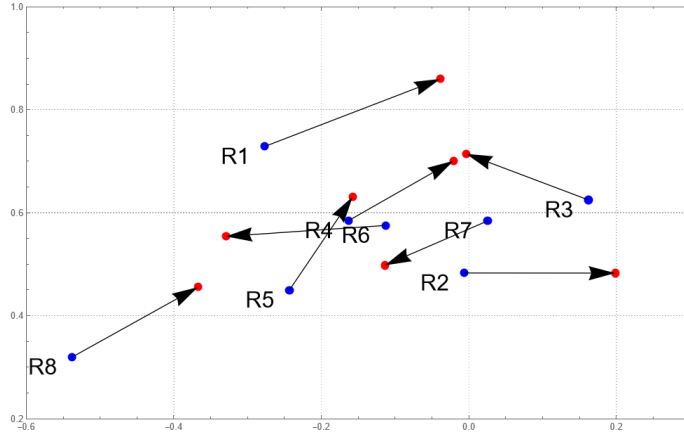


Figure 8: Evolution of the couple $(H_{min}, c_1(p))$ with $p = 1$ deduced from the 1-spectrum of the heart rate between the beginning (in blue) and the end (in red) of the marathon: the evolutions are similar except for three runners: R3 and R6 who had great difficulties and R7 who is the least experienced runner with a much longer running time.

described in Prop. 4 and we conclude in the absence of oscillating singularities at almost every point. This result also shows that $c_1(p)$, which may depend on the value of p (see [67] where it is shown that it is the case for lacunary wavelet series), is intrinsic for such data. We will see in Section 3.5 that a bivariate analysis allows to investigate further in the nature of the pointwise singularities of the data.

We now consider the evolution of the multifractality parameters during a marathon: at about the 25th Km (circa 60 % of the race) runners feel an increased penibility on the RPE Borg scale. Therefore we expect to find two regimes with different parameters before and after this moment. This is put in evidence by Fig. 8 which shows the evolution of the multifractality parameters during the first half and the last fourth of the marathon thus putting in evidence the different physiological reactions at about the 28th Km. From the evolution of the multifractal parameters between the beginning and the end of the marathon

race, we can distinguish between the less experimented marathon runners, whichever their level of fitness, and those who know how to self pace their race. Indeed, according to the evolution of the couple $(h_f^{min}, c_1(p))$, the less experimented (R 7) loosed the regularity of his heart rate variation. This shows that the mararathon running experience allows to feel how to modulate the speed for a conservative heart rate variability. From the evolution of the multifractal parameters between the beginning and the end of the marathon race, we can distinguish between the less experimented marathon runners, whichever their level of fitness and those who know how to self pace their race. In [102] its was shown that the best marathon performance was achieved with a speed variation between extreme values. Furthermore, a phsyiological steady state (heart rate and other cardiorespiratory variables), are obtained with pace variation [32]. This conclusion is in opposition with the less experimented runners beliefs that the constant pace is the best, following the mainstream non scientific basis recommendations currently available on internet.

In Section 3.5 we will investigate the additional information which is revealed by the joint analysis of several physiological data.

3 Multivariate multifractal analysis

Up to now, in most applications, multifractal analysis was performed in univariate settings, (see a contrario [89]), which was mostly due to a lack of theoretical foundations and practical analysis tools. Our purpose in this section is to provide a comprehensive survey of the recent works that started to provide these foundations, and to emphasize the mathematical questions which they open. In particular, multivariate spectra also encode on specific data construction mechanisms. Multivariate multifractal analysis deals with the joint multifractal analysis of several functions. For notational simplicity, we assume in the following that we deal with two functions f_1 and f_2 defined on \mathbb{R}^d and that, to each function is associated a pointwise regularity exponent $h_1(x)$ and $h_2(x)$ (which need not be the same).

3.1 Multivariate spectrum

On the mathematical side, the main issue is to understand how the isoregularity sets

$$E_{f_1}(H_1) = \{x : h_1(x) = H_1\} \quad \text{and} \quad E_{f_2}(H_2) = \{x : h_2(x) = H_2\}$$

of each function are “related”. A natural way to translate this loose question into a precise mathematical problem is to ask for the determination of the *multivariate multifractal spectrum* defined as the two-variables function

$$\mathcal{D}_{(f_1, f_2)}(H_1, H_2) = \dim(\{x : h_1(x) = H_1 \text{ and } h_2(x) = H_2\}). \quad (47)$$

this means that we want to determine the dimension of the intersection of the two isoregularity sets $E_{f_1}(H_1)$ and $E_{f_2}(H_2)$. The determination of the dimension of the intersection of two fractal sets usually is a difficult mathematical question, with no general results available, and it follows that few multivariate spectra have been determined mathematically, see e.g. [24, 25] for a joint analysis of invariant measures of dynamical systems. One can also

mention correlated and anticorrelated binomial cascades, see Section 3.4 for the definition of these cascades, and [76] for the determination of bivariate spectra when two of these cascades are considered jointly.

On the mathematical side, two types of results often show up. A first category follows from the intuition supplied by intersections of smooth manifolds: In general, two surfaces in \mathbb{R}^3 intersect along a curve and, more generally, in \mathbb{R}^d , manifolds intersect *generically* according to the *sum of codimensions rule*:

$$\dim(A \cap B) = \min(\dim A + \dim B - d, -\infty)$$

(i.e. the “codimensions” $d - \dim A$ and $d - \dim B$ add up except if the output is negative, in which case we obtain the emptyset). This formula is actually valid for numerous examples of fractal sets, in particular when the Hausdorff and Packing dimensions of one of the sets A or B coincide (e.g. for general Cantor sets) [95]; in that case “generically” has to be understood in the following sense: For a subset of positive measure among all rigid motions σ , $\dim(A \cap \sigma(B)) = \min(\dim A + \dim B - d, -\infty)$. However the coincidence of Hausdorff and Packing dimensions needs not be satisfied by isoregularity sets, so that such results cannot be directly applied for many mathematical models. The only result that holds in all generality is the following: if A and B are two Borel subsets of \mathbb{R}^d , then, for a generic set of rigid motions σ , $\dim(A \cap \sigma(B)) \geq \dim A + \dim B - d$. This leads to a first rule of thumb for multivariate multifractal spectra: When two functions are randomly shifted, then their singularity sets will be in “generic” position with respect to each other, yielding

$$\mathcal{D}_{(f_1, f_2)}(H_1, H_2) \geq \mathcal{D}_{f_1}(H_1) + \mathcal{D}_{f_2}(H_2) - d.$$

In practice, this result suffers from two limitations: the first one is that, usually, one is not interested in randomly shifted signals but on the opposite for particular configurations where we expect the conjunction of singularity sets to carry relevant information. Additionally, for large classes of fractal sets, the *sets with large intersection*, the codimension formula is not optimal as they satisfy

$$\dim(A \cap B) = \min(\dim A, \dim B).$$

While this alternative formula may seem counterintuitive, general frameworks where it holds were uncovered, cf. e.g., [44, 42, 21] and references therein. This is notably commonly met by *limsup sets*, obtained as follows: There exists a collection of sets A_n such that A is the set of points that belong to an infinite number of the A_n . This is particularly relevant for multifractal analysis where the singularity sets E_H^- defined in (45) often turn out to be of this type: It is the case for Lévy processes or random wavelet series, see e.g. [60, 14, 58]. For multivariate multifractal spectra, this leads to an alternative formula

$$\mathcal{D}_{(f_1, f_2)} = \min(\mathcal{D}_{f_1}(H_1), \mathcal{D}_{f_2}(H_2)) \tag{48}$$

expected to hold in competition with the codimension formula, at least for the sets E_H^- . The existence of two well motivated formulas in competition makes it hard to expect that general mathematical results could hold under fairly reasonable assumptions. Therefore,

we now turn towards the construction of multifractal formalisms adapted to a multivariate setting, first in order to inspect if this approach can yield more intuition on the determination of multivariate spectra and, second, in order to derive new multifractality parameters which could be used for model selection and identification, and also in order to get some understanding on the ways that singularity sets of several functions are correlated.

In order to get some intuition in that direction, it is useful to start with a probabilistic interpretation of the multifractal quantities that were introduced in the univariate setting.

3.2 Probabilistic interpretation of scaling functions

We consider the following probabilistic toy-model: We assume that, for a given j , the wavelet coefficients $(c_{j,k})_{k \in \mathbb{Z}}$ of the signal considered share a common law X_j and display short range memory, i.e. become quickly decorrelated when the wavelets $\psi_{j,k}$ and $\psi_{j,k'}$ are located far away (i.e. when $k - k'$ gets large); then, the wavelet structure functions (27) can be interpreted as an empirical estimation of $\mathbb{E}(|X_j|^p)$, i.e. the moments of the random variables X_j , and the wavelet scaling function characterizes the power law behaviour of these moments (as a function of the scale 2^{-j}). This interpretation is classically acknowledged for signals which display some stationarity, and the vanishing moments of the wavelets reinforce this decorrelation even if the initial process displays long range correlations, see e.g. the studies performed on classical models such as fBm ([1] and ref. therein). We will not discuss the relevance of this model; we just note that this interpretation has the advantage of pointing towards probabilistic tools when one shifts from one to several signals, and these tools will allow to introduce natural classification parameters which can then be used even when the probabilistic assumptions which led to their introduction have no reason to hold.

From now on, we consider two signals f_1 and f_2 defined on \mathbb{R} (each one satisfying the above assumptions) with wavelet coefficients respectively $c_{j,k}^1$ and $c_{j,k}^2$. The “covariance” of the wavelet coefficients at scale j is estimated by the empirical correlations

$$\text{for } m, n = 1, 2, \quad S_{m,n}(j) = 2^{-j} \sum_k c_{j,k}^m c_{j,k}^n. \quad (49)$$

Log-log regressions of these quantities (as a function of $\log(2^{-j})$) allow to determine if some power-law behaviour of these auto-correlations (if $m = n$) and cross-correlations (if $m \neq n$) can be put in evidence: When these correlations are found to be significantly non-negative, one defines the *scaling exponents* $H_{m,n}$ implicitly by

$$S_{m,n}(j) \sim 2^{-H_{m,n}j}$$

in the limit of small scales. Note that, if $m = n$, the exponent associated with the auto-correlation simply is $\eta_f(2)$ and is referred to as the *Hurst exponent* of the data.

Additionally, the *wavelet coherence function* is defined as

$$C_{1,2}(j) = \frac{S_{1,2}(j)}{\sqrt{S_{1,1}(j)S_{2,2}(j)}}.$$

It ranges within the interval $[-1, 1]$ and quantifies, as a scale-dependent correlation coefficient, which scales are involved in the correlation of the two signals, see [4, 115].

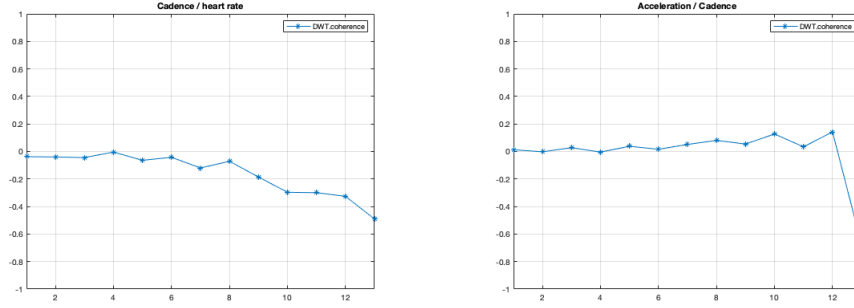


Figure 9: Wavelet coherence between heart-beat frequency and cadence (left) and between acceleration and cadence (right).

Note that probabilistic denominations such as “auto-correlation”, “cross-correlations” and “coherence function” are used even if no probabilistic model is assumed, and used in order to derive scaling parameters obtained by log-log plot regression which can prove powerful as classification tools.

As an illustration, we estimated these crosscorrelations concerning the following couples of data recorded on marathon runners: heart-beat frequency vs. cadence, and cadence vs. acceleration, see Fig. 9. In both cases, no correlation between the wavelet coefficients at a given scale is put in evidence. Therefore, this is a situation where the additional bonus brought by measuring multifractal correlations is needed. Indeed, if the cross-correlations of the signals do not carry substantial information, this does not imply that the singularity sets of each signal are not related (as shown by the example supplied by *Brownian motions in multifractal time*, see below in Section 3.4). In that case, a natural idea is to look for correlations that would be revealed by the multiscale quantities associated with pointwise exponents rather than by wavelet coefficients.

3.3 Multivariate multifractal formalism

The idea that leads to a multivariate multifractal formalism is quite similar as the one which led us from wavelet scaling functions to leaders and p -leaders scaling functions: One should incorporate in the cross-correlations the multiscale quantities which allow to characterize pointwise regularity, i.e. replace wavelet coefficients by wavelet leaders in (49).

Suppose that two pointwise regularity exponents h_1 and h_2 defined on \mathbb{R} are given. We assume that each of these exponents can be derived from corresponding multiresolution quantities $d_{j,k}^1$, and $d_{j,k}^2$ according to (31). A *grandcanonical multifractal formalism* allows to estimate the joint spectrum $\mathcal{D}(H_1, H_2)$ of the couple of exponents (h_1, h_2) as proposed in [96]. In the general setting provided by multiresolution quantities, it is derived as follows: The *multivariate structure functions* associated with the couple $(d_{j,k}^1, d_{j,k}^2)$ are defined by

$$\forall r = (r_1, r_2) \in \mathbb{R}^2, \quad S(r, j) = 2^{-j} \sum_k (d_{j,k}^1)^{r_1} (d_{j,k}^2)^{r_2}, \quad (50)$$

see [6, 28] for the seminal idea of proposing such multivariate multiresolution quantities as building blocks of a *grandcanonical formalism*. Note that they are defined as a cross-correlation, which would be based on the quantities $d_{j,k}^1$ and $d_{j,k}^2$, with the extra flexibility of raising them to arbitrary powers, as is the case for univariate structure functions. The corresponding *bivariate scaling function* is

$$\zeta(r) = \liminf_{j \rightarrow +\infty} \frac{\log(S(r, j))}{\log(2^{-j})}. \quad (51)$$

The *bivariate Legendre spectrum* is obtained through a 2-variable Legendre transform

$$\forall H = (H_1, H_2) \in \mathbb{R}^2, \quad \mathcal{L}(H) = \inf_{r \in \mathbb{R}^2} (1 - \zeta(r) + H \cdot r), \quad (52)$$

where $H \cdot r$ denotes the usual scalar product in \mathbb{R}^2 . Apart from [96], this formalism has been investigated in a wavelet framework for joint Hölder and oscillation exponents in [9], in an abstract general framework in [101], and on wavelet leader and p -leader based quantities in [67, 6].

Remark: The setting supplied by orthonormal wavelet bases is well fitted to be extended to the multivariate setting, because the multiresolution quantities d_λ are defined on a preexisting (dyadic) grid, which is shared by both quantities. Note that this is not the case for the WTMM, where the multiresolution quantities are defined at the local maxima of the continuous wavelet transform (see (17)), and these local maxima differ for different signals; thus, defining multivariate structure functions in this setting would lead to the complicated questions of matching these local maxima correctly in order to construct bivariate structure functions similar to (50).

The multivariate multifractal formalism is backed by only few mathematical results. A first reason is that, as already mentioned, the Legendre spectrum does not yield in general an upper bound for the multifractal spectrum, and this property is of key importance in the univariate setting. Another drawback is that, in constradistinction with the univariate case, the scaling function (51) has no function space interpretation. It follows that there exists no proper setting for genericity results except if one defines a priori this function space setting (as in [28, 27] where generic results are obtained in couples of function spaces endowed with the natural norm on a product space). We meet here once again the problem of finding a “proper” genericity setting that would be fitted to the quantities supplied by scaling functions. We now list several positive results concerning multivariate Legendre spectra.

The following result of [77] shows how to recover the univariate Legendre spectra from the bivariate one.

Proposition 5 *Let $d_{j,k}^1$, and $d_{j,k}^2$ be two multiresolution quantities associated with two point-wise exponents $h_1(x)$ and $h_2(x)$. The associated uni- and bi-variate Legendre spectra are related as follows:*

$$\mathcal{L}_1(H_1) = \sup_{H_2} \mathcal{L}(H_1, H_2) \quad \text{and} \quad \mathcal{L}_2(H_2) = \sup_{H_1} \mathcal{L}(H_1, H_2).$$

This property implies that results similar to Theorem 1 hold in the multivariate setting.

Corollary 1 *Let $d_{j,k}^1$ and $d_{j,k}^2$ be two multiresolution quantities associated with two pointwise exponents $h_1(x)$ and $h_2(x)$. The following results on the couple $(h_1(x), h_2(x))$ hold:*

- *If the bivariate Legendre spectrum has a unique maximum for $(H_1, H_2) = (c_1, c_2)$, then*

$$\text{for almost every } x, \quad h_1(x) = c_1 \quad \text{and} \quad h_2(x) = c_2. \quad (53)$$

- *If the leader scaling function is affine then*

$$\exists(c_1, c_2), \quad \forall x, \quad h_1(x) = c_1 \quad \text{and} \quad h_2(x) = c_2.$$

Note that the fact that the leader scaling function is affine is equivalent to the fact that the bivariate Legendre spectrum is supported by a point. In that case, if the exponents h_1 and h_2 are associated with the functions f_1 and f_2 , then they are monohölder functions.

Proof: The first point holds because, if the bivariate Legendre spectrum has a unique maximum, then, its projections on the H_1 and the H_2 axes also have a unique maximum at respectively $H_1 = c_1$ and $H_2 = c_2$ and Proposition 5 together with Theorem 1 imply (53).

As regards the second statement, one can use Proposition 5: If the bivariate scaling function is affine, then $\mathcal{L}(H_1, H_2)$ is supported by a point, so that Proposition 5 implies that it is also the case for univariate spectra $\mathcal{L}(H_1)$ and $\mathcal{L}(H_2)$, and Theorem 1 then implies that h_1 is constant and the same holds for h_2 .

Recall that, in general, the bivariate Legendre spectrum does not yield an upper bound for the multifractal spectrum (in contradistinction with the univariate case), see [76] where a counterexample is constructed; this limitation raises many open questions: Is there another way to construct a Legendre spectrum which would yield an upper bound for $\mathcal{D}(H_1, H_2)$? which information can actually be derived from the Legendre spectrum? A first positive result was put in light in [76], where a notion of “compatibility” between exponents is put in light and is shown to hold for several models: When this property holds, then the upper bound property is satisfied. It is not clear that there exists a general way to check directly on the data if it is satisfied; however, an important case where it is the case is when the exponents derived are the Hölder exponent and one of the “second generation exponents” that we mentioned, see [67, 6]. In that case, the upper bound property holds, and it allows to conclude that the signal does not display e.g. oscillating singularities, an important issue both theoretical and practical. Let us mention a situation where this question shows up: In [19], P. Balanca showed the existence of oscillating singularities in the sample of some Lévy processes and also showed that they are absent in others (depending on the Lévy measure which is picked in the construction); however, he only worked out several examples, and settling the general case is an important issue; numerical estimations of such bivariate spectra could help to make the right conjectures in this case.

The general results listed in Corollary 1 did not require assumptions on correlations between the exponents h_1 and h_2 . We now investigate the implications of such correlations

on the joint Legendre spectrum. For that purpose, let us come back to the probabilistic interpretation of the structure functions (50) in terms of cross-correlation of the $(d_{j,k}^1)^{r_1}$ and $(d_{j,k}^2)^{r_2}$. As in the univariate case, if we assume that, for a given j , the multiresolution quantities $d_{j,k}^1$ and $d_{j,k}^2$ respectively share common laws X_j^1 and X_j^2 and display short range memory, then (50) can be interpreted as an empirical estimation of $\mathbb{E}(|X_j^1|^{r_1}|X_j^2|^{r_2})$. If we additionally assume that the $(d_{j,k}^1)$ and $(d_{j,k}^2)$ are independent, then we obtain

$$S(r, j) = \mathbb{E}(|X_j^1|^{r_1}|X_j^2|^{r_2}) = \mathbb{E}(|X_j^1|^{r_1}) \cdot \mathbb{E}(|X_j^2|^{r_2}),$$

which can be written

$$S(r_1, r_2, j) = S^1(r_1, j)S^2(r_2, j). \quad (54)$$

Assuming that \liminf in (51) actually is a limit, we obtain $S(r_1, r_2, j) \sim 2^{-(\zeta^1(r_1) + \zeta^2(r_2))j}$ yielding $\zeta(r_1, r_2) = \zeta^1(r_1) + \zeta^2(r_2)$. Applying (52), we get

$$\begin{aligned} \mathcal{L}(H_1, H_2) &= \inf_{(r_1, r_2) \in \mathbb{R}^2} (1 - \zeta^1(r_1) + \zeta^2(r_2) + H_1 r_1 + H_2 r_2) \\ &= \inf_{r_1} (1 - \zeta^1(r_1) + H_1 r_1) + \inf_{r_2} (1 - \zeta^2(r_2) + H_2 r_2) - 1, \end{aligned}$$

which leads to

$$\mathcal{L}(H_1, H_2) = \mathcal{L}(H_1) + \mathcal{L}(H_2) - 1. \quad (55)$$

Thus, under stationarity and independence, the codimension rule applies for the multivariate Legendre spectrum. In practice, this means that any departure of the Legendre spectrum from (55), which can be checked on real-life data, indicates that one of the assumptions required to yield (55) (either stationarity or independence) does not hold.

As a byproduct, we now show that multivariate multifractal analysis can give information on the nature of the singularities of *one* signal, thus complementing results such as Proposition 4 which yielded almost everywhere information of this type. Let us consider the joint multifractal spectrum of a function f and its fractional integral of order s , denoted by $f^{(-s)}$. If f only has canonical singularities, then the Hölder exponent of $f^{(-s)}$ satisfies $\forall x_0, h_{f^{(-s)}}(x_0) = h_f(x_0) + s$, so that the joint Legendre spectrum is supported by the line $H_2 = H_1 + s$. In that case, the synchronicity assumption is satisfied and one can conclude that the joint multifractal spectrum is supported by the same segment; a contrario, a joint Legendre spectrum which is not supported by this line is interpreted as the signature of *oscillating singularities* in the data, as shown by the discussion above concerning the cases where the upper bound for bivariate spectra holds. Figs. 11, 12 and 13 illustrate this use of bivariate multifractal analysis: In each case, a signal and its primitive are jointly analyzed: The three signals are collected on the same runner and the whole race is analyzed. Fig. 11 shows the analysis of heartbeat, Fig. 12 shows the cadence and Fig. 13 shows the acceleration. In the first case, the analysis is performed directly on the data using a p -exponent with $p = 1$, whereas, for the two last ones, the analysis is performed on a fractional integral of order $1/2$. In each case, the results yield a bivariate Legendre spectrum supported by the segment $H_2 = H_1 + s$, which confirms the almost everywhere results obtained in Section 2.9: The data only contain canonical singularities.

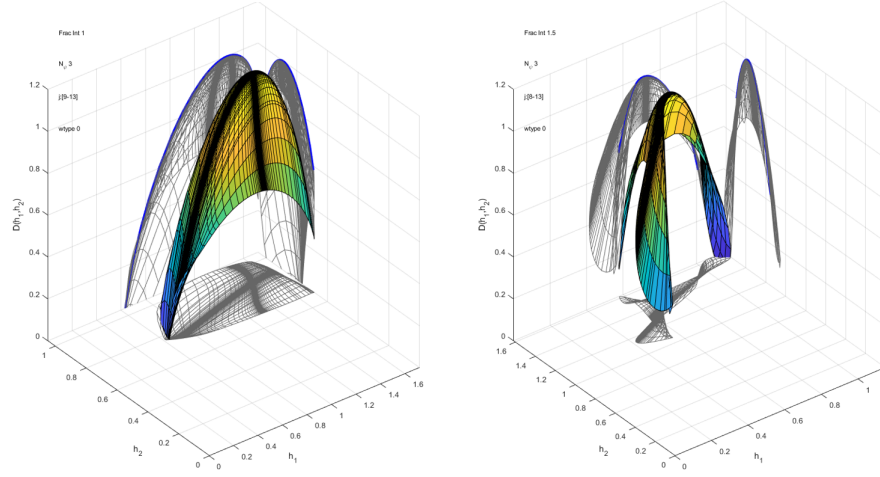


Figure 10: On the left, the bivariate multifractal spectrum between heart-beat frequency primitive and cadence primitive are shown, and, on the right, the bivariate multifractal spectrum between acceleration and cadence with fractional integral of order 1.5 are shown. This demonstrates the strong correlation between the pointwise singularities of the two data: indeed the bivariate spectra are almost carried by a segment, and a bivariate spectrum carried by a line $H_2 = aH_1 + b$ indicates a perfect match between the pointwise exponents according to the same relationship: $\forall x, h_2(x) = ah_1(x) + b$

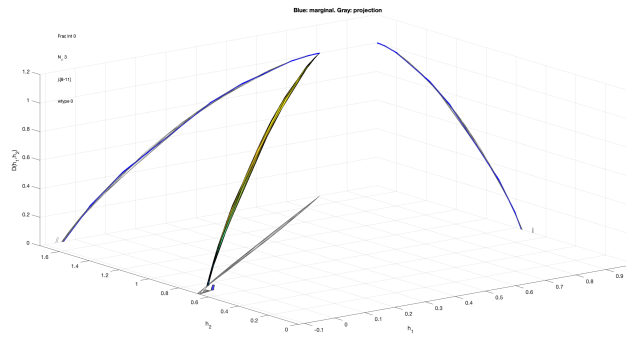


Figure 11: Bivariate 1-spectrum of heartbeat frequency and its primitive: the bivariate spectrum lines up perfectly along the line $H_2 = H_1 + 1$.

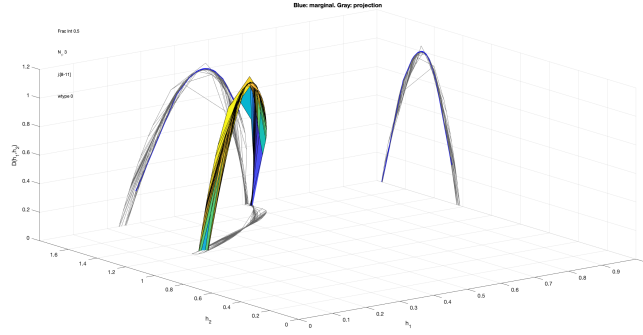


Figure 12: Bivariate Hölder spectrum of fractional integrals order $1/2$ and $3/2$ of cadence: the bivariate spectrum lines up perfectly along the line $H_2 = H_1 + 1$.

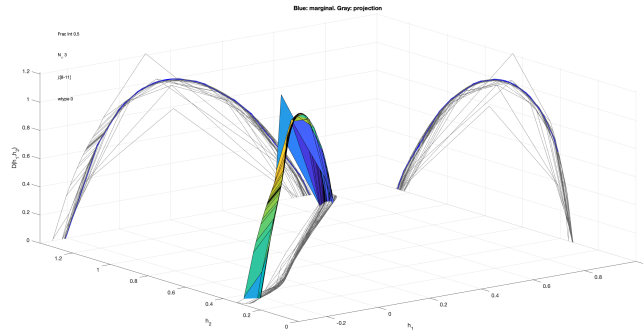


Figure 13: Bivariate Hölder spectrum of fractional integrals of order $1/2$ and $3/2$ of acceleration: the bivariate spectrum lines up perfectly along the line $H_2 = H_1 + 1$.

3.4 Fractional Brownian motions in multifractal time

In order to put in light the additional information between wavelet correlations and bivariate scaling functions (and the associated Legendre spectrum), we consider the model supplied by Brownian motion in multifractal time, which has been proposed by B. Mandelbrot [91, 38] as a simple model for financial time series: Instead of the classical Brownian model $B(t)$, he introduced a time change (sometimes referred to as a *subordinator*)

$$B(f(t)) = (B \circ f)(t)$$

where the irregularities of f model the fluctuations of the intrinsic “economic time”, and typically is a multifractal function. In order to be a “reasonable” time change, the function f has to be continuous and strictly increasing; such functions usually are obtained as distribution functions of probability measures $d\mu$ supported on \mathbb{R} (or on an interval), and which have no atoms (i.e. $\forall a \in \mathbb{R}, \mu(a) = 0$); typical examples are supplied by deterministic or random cascades, and this is the kind of models that were advocated by B. Mandelbrot in [91]. Such examples will allow to illustrate the different notions that we introduced, and the additional information which is put into light by the bivariate Legendre spectrum and is absent from wavelet correlations.

Let us consider the slightly more general setting of one fBm of Hurst exponent α (the cas of Brownian motion corresponds to $\alpha = 1/2$) modified by a time change f . In order to simplify its theoretical multifractal analysis, we take for pointwise regularity exponent the Hölder exponent and we make the following assumptions of f : We assume that it has only canonical singularities and that, if they exist, the non-constant terms of the Taylor polynomial of f vanish at every point even if the Hölder exponent at some points is larger than 1 (this is typically the case for primitives of singular measures). In that case, classical uniform estimates on increments of fBm, see [79] imply that

$$\text{a.s.} \quad \forall t, \quad h_{B \circ f}(t) = \alpha h_f(t), \quad (56)$$

so that

$$\text{a.s.} \quad \forall H, \quad \mathcal{D}_{B \circ f}(H) = \mathcal{D}_f(H/\alpha);$$

Note that the simple conclusion (56) may fail if the Taylor polynomial is not constant at every point, as shown by the simple example supplied by $f(x) = x$ on the interval $[0, 1]$.

We now consider $B_1 \circ f$ and $B_2 \circ f$: two independent fBm modified by the *same deterministic time change* f (with the same assumptions as above). It follows from (56) that, with probability 1, the Hölder exponents of $B_1 \circ f$ and $B_2 \circ f$ coincide everywhere, leading to the following multifractal spectrum, which holds almost surely:

$$\begin{cases} \text{if } H_1 = H_2, & \mathcal{D}_{(B_1 \circ f, B_2 \circ f)}(H_1, H_2) = \mathcal{D}_f\left(\frac{H_1}{\alpha}\right) \\ \text{if } H_1 \neq H_2, & \mathcal{D}_{(B_1 \circ f, B_2 \circ f)}(H_1, H_2) = -\infty. \end{cases} \quad (57)$$

Fig. 17 gives a numerical backing of this result: The Legendre spectrum numerically obtained corresponds to the theoretical multifractal spectrum. Let us give a non-rigorous

argument which backs this result: The absence of oscillating singularities in the data implies that the maxima in the wavelet leaders are attained for a λ' close to λ , so that the wavelet leaders of a given magnitude will be close to coincide for both processes, and therefore the bivariate structure functions (50) satisfy

$$S_f(r, j) = 2^{-j} \sum_{\lambda \in \Lambda_j} (d_\lambda^1)^{r_1} (d_\lambda^2)^{r_2} \sim 2^{-dj} \sum_{\lambda \in \Lambda_j} (d_\lambda^1)^{r_1+r_2}$$

so that

$$\text{a.s. , } \quad \forall r_1, r_2, \quad \tilde{\zeta}(r_1, r_2) = \zeta(r_1 + r_2).$$

where $\tilde{\zeta}$ is the bivariate scaling function of the couple $(B_1 \circ f, B_2 \circ f)$ and ζ is the univariate scaling function of $B_1 \circ f$. Taking a Legendre transform yields that the bivariate Legendre spectrum $\mathcal{L}(H_1, H_2)$ also satisfies a similar formula as (57), i.e.

$$\text{a.s. , } \quad \forall H_1, H_2, \quad \begin{cases} \text{if } H_1 = H_2, & \mathcal{L}_{(B_1 \circ f, B_2 \circ f)}(H_1, H_2) = \mathcal{L}_f\left(\frac{H_1}{\alpha}\right) \\ \text{if } H_1 \neq H_2, & \mathcal{L}_f(H_1, H_2) = -\infty. \end{cases} \quad (58)$$

Let us now estimate the wavelet cross correlations. Since f is deterministic, the processes $B_1 \circ f$ and $B_2 \circ f$ are two independent centered Gaussian processes. Their wavelet coefficients $c_{j,k}^1$ and $c_{j,k}^2$ therefore are independent centered Gaussians, and, at scale j the quantity

$$S_{m,n}(j) = 2^{-j} \sum_k c_{j,k}^1 c_{j,k}^2$$

is an empirical estimation of their covariance, and therefore vanishes (up to small statistical fluctuation). In contradistinction with the bivariate spectrum, the wavelet cross correlations reveal the decorrelation of the processes but does not yield information of the correlation of the singularity sets.

In order to illustrate these results, we will use for time change the distribution function of a binomial cascade μ_p carried on $[0, 1]$. Let $p \in (0, 1)$; μ_p is the only probability measure on $[0, 1]$ defined by recursion as follows: Let $\lambda \subset [0, 1]$ be a dyadic interval of length 2^{-j} ; we denote by λ^+ and λ^- respectively its two “children” of length 2^{-j-1} , λ^+ being on the left and λ^- being on the right. Then, μ_p is the only probability measure carried by $[0, 1]$ and satisfying

$$\mu_p(\lambda^+) = p \cdot \mu_p(\lambda) \quad \text{and} \quad \mu_p(\lambda^-) = (1 - p) \cdot \mu_p(\lambda).$$

Then the corresponding time change is the function

$$\forall x \in [0, 1] \quad f_{\mu_p}(x) = \mu_p([0, x]).$$

In Fig. 14, we show the binomial cascade $\mu_{1/4}$ and its distribution function, and in Fig. 16 we use this time change composed with a fBm of Hurst exponent $\alpha = 0.3$.

Remarks: The fact that the same time change is performed does not play a particular role for the estimation of the wavelet cross-correlations; the same result would follow for two processes $B_1 \circ f$ and $B_2 \circ g$ with B_1 and B_2 independent, and where f and g are two

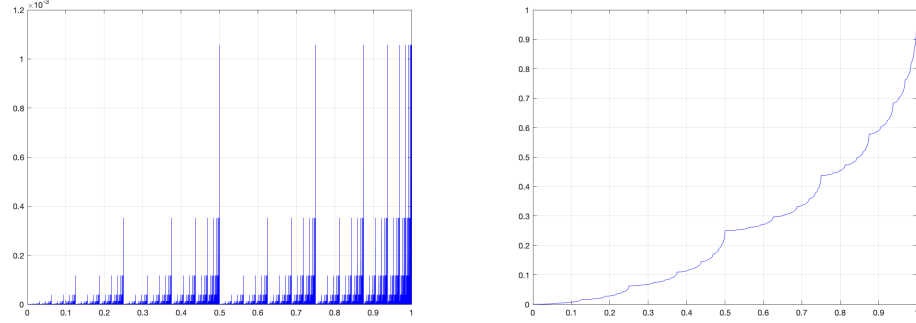


Figure 14: Binomial measure with $p = 1/4$ (left) and its repartition function (right) which is used as the time change in Fig. 16.

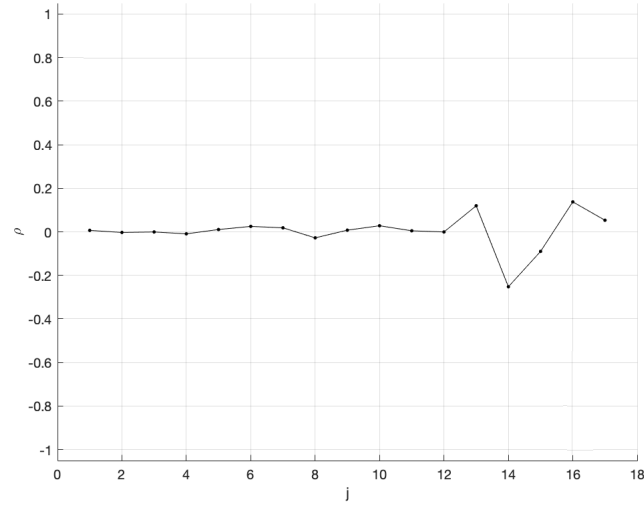


Figure 15: Cross-correlation of the wavelet coefficients of two independent fBm with the same time change : the distribution function of the binomial measure μ_p with $p = 1/4$. The Cross-correlation reflects the independence of the two processes.

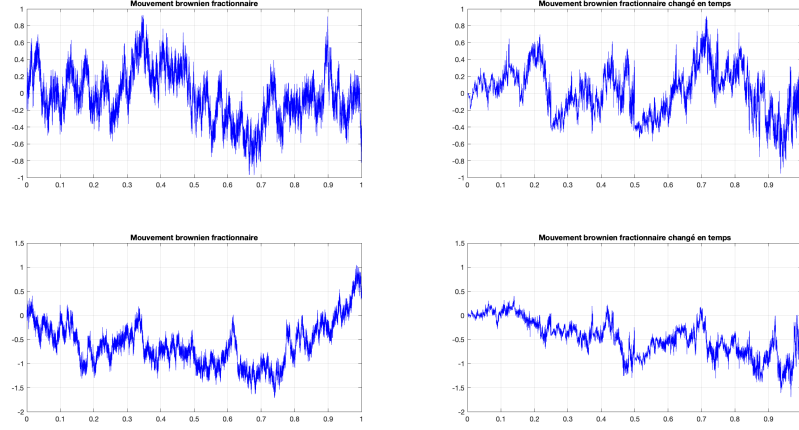


Figure 16: fBm with $H = 0.3$ subordinated by the multifractal time change supplied by the distribution function of the binomial measure μ_p with $p = 1/4$.

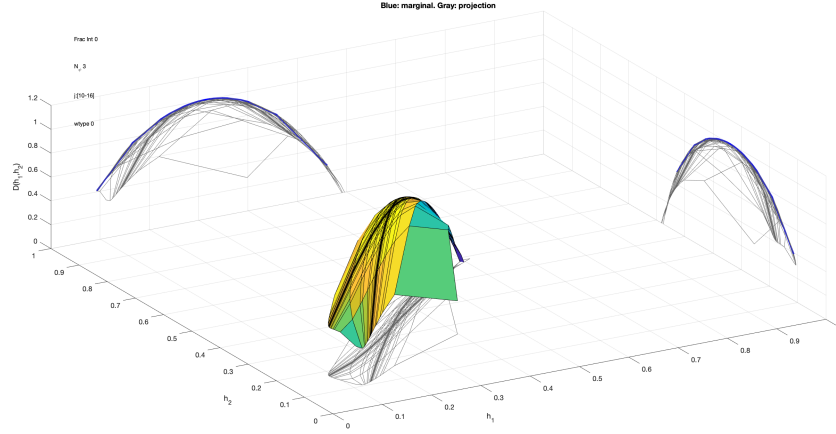


Figure 17: Bivariate multifractal spectrum of two independent fBm with the same time change: the distribution function of a binomial measure with $p = 1/4$; in contradistinction with the cross-correlation of wavelet coefficients, the wavelet leaders are strongly correlated, leading to a bivariate Legendre spectrum theoretically supported by the line $H_1 = H_2$, which is close to be the case numerically.

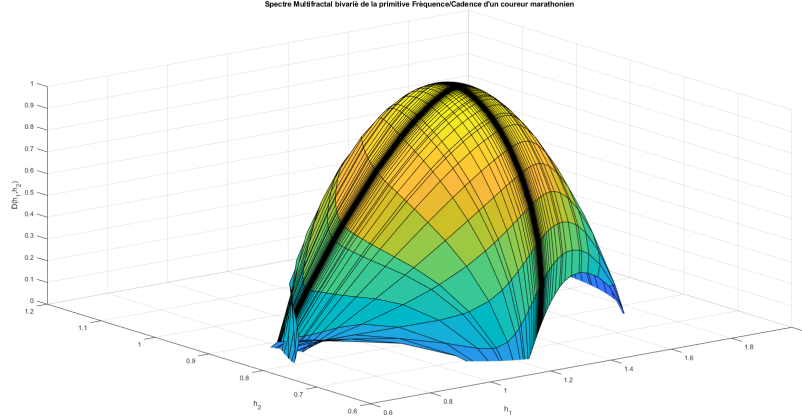


Figure 18: Representation of the bivariate Hölder Legendre spectrum of the primitives of heart beat frequency and cadence: this bivariate spectrum is derived from the same data that were used to derive the two univariate spectra shown in Fig 5.

deterministic time changes. Similarly, B_1 and B_2 can be replaced by two (possibly different) centered Gaussian processes.

Let us mention at this point that the mathematical problem of understanding what is the multifractal spectrum of the composition $f \circ g$ of two multifractal functions f and g , where g is a *time subordinator* i.e. an increasing function, is a largely open problem (and is posed here in too much generality to find a general answer). This problem was initially raised by B. Mandelbrot and also investigated R. Riedi [103] who worked out several important subcases; see also the article by S. Seuret [105], who determined a criterium under which a function can be written as the composition of a time subordinator and a monohölder function, and [22] where J. Barral and S. Seuret studied the multifractal spectrum of a Lévy process, under a time subordinator given by the repartition function of a multifractal cascade.

3.5 Multivariate analysis of marathon physiological data

Let us consider one of the marathon runners, and denote his heart beat frequency by f_f and his cadence by f_c and by $f_f^{(-1)}$ and $f_c^{(-1)}$ their primitives. We performed the computation of the bivariate scaling function $\zeta_{f_f^{(-1)}, f_c^{(-1)}}$ (using wavelet leaders) and we show its Legendre transform $\mathcal{L}_{f_f^{(-1)}, f_c^{(-1)}}$ on Fig. 18. This spectrum is widely spread, in strong contradistinction with the bivariate spectra obtained in the previous section; this indicates that no clear correlations between the Hölder singularities of the primitives can be put in evidence. Fig. 5 shows the two corresponding univariate spectra (which can be either computed directly, or obtained as projections of the bivariate spectrum).

In order to test possible relationships between the bivariate spectrum and the two cor-

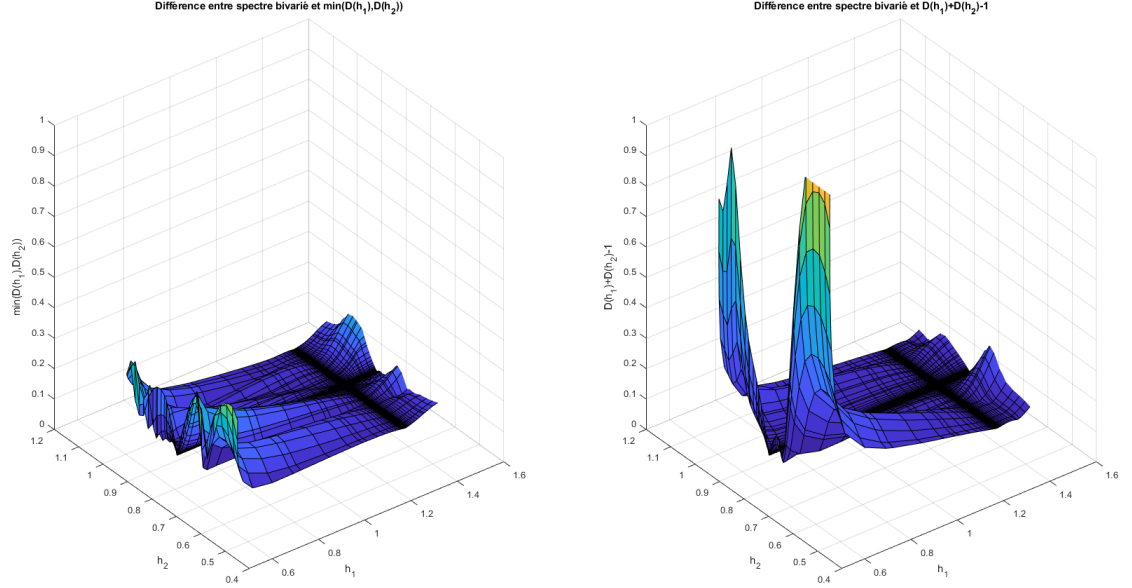


Figure 19: Representation of the difference of the bivariate spectrum and the two formulas proposed in (55) and (48). The graph on the left is closer to zero, which suggests that the large intersection formula seems more appropriate in this case.

responding univariate spectra, we compute the difference

$$\mathcal{L}(H_1, H_2) - \mathcal{L}(H_1) - \mathcal{L}(H_2) + 1,$$

which allows to test the validity of (55) and

$$\mathcal{L}_{(f_1, f_2)} - \min(\mathcal{L}_{f_1}(H_1), \mathcal{L}_{f_2}(H_2)),$$

which allows to test the validity of (48), they are shown in Fig. 19. This comparison suggests that the large intersection formula is more appropriate than the codimension formula in this case. Keeping in mind the conclusions of Section 3.1, these results indicate that an hypothesis of both stationarity and independence for each signals is inappropriate (indeed this would lead to the validity of the codimension formula), and on the opposite, these results are compatible with a pointwise regularity yielded by a limsup set procedure, as explained in Sec 3.1.

4 Conclusion

Let us give a summary of the conclusions that can be drawn from a bivariate multifractal analysis of data based on the Legendre transform method. This analysis goes beyond the

(now standard) technique of estimating correlations of wavelet coefficients; indeed here wavelet coefficients are replaced by wavelet leaders, which leads to new scaling parameters on which classification can be performed. On the mathematical side, even if the relationship between the Legendre and the multifractal spectra is not as clear as in the univariate case, nonetheless, situations have been identified where this technique can either yield information on the nature of the singularities (e.g. the absence of oscillating singularities), or on the type of processes that can be used to model the data (either of additive or of multiplicative type). In the particular case of marathon runners, the present study shows a bivariate spectra between heart rate and cadence are related by the large intersection formula. In a recent study [32] a multivariate analysis revealed that, for all runners, RPE and respiratory frequency measured on the same runners during the marathon were close (their angle is acute on correlation circle of a principal component analysis) while the speed was closer to the cadence and to the Tidal respiratory volume at each inspiration and expiration). The sampling frequency of the respiratory parameters did not allow to apply the multifractal analysis which here reveals that the cadence and heart rate could be an additive process such as, possibly a generalization of a Lévy process. Heart rate and cadence are under the autonomic nervous system control and Human beings optimize their cadence according his speed for minimizing his energy cost of running. Therefore, we can conclude that is not recommended to voluntarily change the cadence and this bivariate multifractal analysis mathematically shows that the cadence and heart rate are not only correlated but we can conjecture that they can be modeled by an additive process until the end of the marathon.

References

- [1] P. Abry, P. Gonçalves, and P. Flandrin. *Wavelets, spectrum estimation and $1/f$ processes*, chapter 103. Springer-Verlag, New York, 1995. Wavelets and Statistics, Lecture Notes in Statistics. [36](#)
- [2] P. Abry, S. Jaffard, and H. Wendt. A bridge between geometric measure theory and signal processing: Multifractal analysis. *Operator-Related Function Theory and Time-Frequency Analysis, The Abel Symposium 2012*, K. Gröchenig et al., Eds., 9:1–56, 2015. [13](#), [15](#), [16](#), [24](#)
- [3] P. Abry, S. Jaffard, and H. Wendt. Irregularities and scaling in signal and image processing: Multifractal analysis. *Benoit Mandelbrot: A Life in Many Dimensions*, M. Frame and N. Cohen, Eds., World scientific publishing, pages 31–116, 2015. [3](#), [10](#), [14](#), [15](#), [19](#), [27](#)
- [4] P. Abry, H. Wendt, S. Jaffard, and G. Didier. Multivariate scale-free temporal dynamics: From spectral (fourier) to fractal (wavelet) analysis. *Comptes Rendus de l’Académie des Sciences*, 20(5):489–501, 2019. [19](#), [36](#)
- [5] P. Abry, H. Wendt, S. Jaffard, H. Helgason, P. Gonçalves, E. Pereira, C. Gharib, P. Gaucherand, and M. Doret. Methodology for multifractal analysis of heart rate

- variability: From lf/hf ratio to wavelet leaders. In *32nd Annual International Conference of the IEEE Engineering in Medicine and Biology, Buenos Aires, Argentina*, 2010. [3](#), [31](#)
- [6] Patrice Abry, Stéphane Jaffard, Roberto Leonarduzzi, Clothilde Melot, and Herwig Wendt. New exponents for pointwise singularity classification. In Stéphane Seuret and Julien Barral, editors, *Recent Developments in Fractals and Related Fields: Proc. Fractals and Related Fields III, 19-26 September 2015, Porquerolles, France*, pages 1–37, 2017. [20](#), [21](#), [22](#), [23](#), [28](#), [38](#), [39](#)
- [7] Patrice Abry, Stéphane Jaffard, and Herwig Wendt. When van gogh meets mandelbrot: Multifractal classification of painting’s texture. *Signal Proces.*, 93(3):554–572, 2013. [3](#)
- [8] A. Arneodo, B. Audit, N. Decoster, J.-F. Muzy, and C. Vaillant. Wavelet-based multifractal formalism: applications to dna sequences, satellite images of the cloud structure and stock market data. *The Science of Disasters; A. Bunde, J. Kropp, H.J. Schellnhuber, Eds. (Springer)*, pages 27–102, 2002. [10](#)
- [9] A. Arneodo, E. Bacry, S. Jaffard, and J.F Muzy. Singularity spectrum of multifractal functions involving oscillating singularities. *J. Fourier analysis and Applications*, 4:159–174, 1998. [19](#), [20](#), [38](#)
- [10] A. Arneodo, E. Bacry, and J.F. Muzy. The thermodynamics of fractals revisited with wavelets. *Physica A*, 213(1-2):232–275, 1995. [10](#)
- [11] A. Arneodo, C. Baudet, F. Belin, R. Benzi, B. Castaing, B. Chabaud, R. Chavarria, S. Ciliberto, R. Camussi, F. Chillà, B. Dubrulle, Y. Gagne, B. Hebral, J. Herweijer, M. Marchand, J. Maurer, J.F. Muzy, A. Naert, A. Noullez, J. Peinke, S.G. Roux, P. Tabeling, W. van der Water, and H. Willaime. Structure functions in turbulence, in various flow configurations, at Reynolds number between 30 and 5000, using extended self-similarity. *Europhys. Lett.*, 34:411–416, 1996. [4](#)
- [12] A. Arneodo, N. Decoster, P. Kestener, and S.G. Roux. A wavelet-based method for multifractal image analysis: from theoretical concepts to experimental applications. In P.W. Hawkes, B. Kazan, and T. Mulvey, editors, *Advances in Imaging and Electron Physics*, volume 126, pages 1–98. Academic Press, 2003. [3](#)
- [13] J.-M. Aubry. On the rate of pointwise divergence of Fourier and wavelet series in L^p . *J. Approx. Theory*, 538:97–111, 2006. [13](#)
- [14] J.M. Aubry and S. Jaffard. Random wavelet series. *Communications In Mathematical Physics*, 227(3):483–514, 2002. [35](#)
- [15] A. Ayache. On the monofractality of many stationary continuous gaussian fields. *Journal of Functional Analysis*, 281, 2021. [29](#)

- [16] A. Ayache and S. Jaffard. Hölder exponents of arbitrary functions. *Revista Matemática Iberoamericana*, 26:77–89, 2010. [23](#)
- [17] J. Yorke B. Hunt, T. Sauer. Prevalence : a translation invariance "almost every" on infinite dimensional spaces. *Bull. Amer. Math. Soc.*, 27(2):217–238, 1992. [7](#), [29](#)
- [18] E. Bacry, A. Kozhemyak, and J.F. Muzy. Multifractal models for asset prices. *Encyclopedia of quantitative finance*, Wiley, 2010. [3](#)
- [19] P. Balanca. Fine regularity of lévy processes and linear (multi)fractional stable motion. *Electron. J. Probability*, 101:1–37, 2014. [22](#), [39](#)
- [20] J.-M. Bardet. Statistical study of the wavelet analysis of fractional brownian motion. *EEE Trans. Inform. Theory*, 48:991–999, 2002. [26](#)
- [21] J. Barral and S. Seuret. A heterogeneous ubiquitous systems in r^d and Hausdorff dimensions. *Bull. Brazilian Math. Soc.*, 38(3):467–515, 2007. [35](#)
- [22] J. Barral and S. Seuret. The singularity spectrum of Lévy processes in multifractal time. *Adv. Math.*, 14(1):437–468, 2007. [47](#)
- [23] J. Barral and S. Seuret. Besov spaces in multifractal environment, and the frisch-parisi conjecture. *preprint*, 2021. [30](#)
- [24] L Barreira and B Saussol. Variational principles and mixed multivariate spectra. *Trans. A. M. S.*, 353 (10):3919–3944, 2001. [34](#)
- [25] L Barreira, B Saussol, and J Schmeling. Higher-dimensional multifractal analysis. *Journal des Mathématiques Pures et Appliquées*, 81:67–91, 2002. [34](#)
- [26] F. Bayart and Y. Heurteaux. Multifractal analysis of the divergence of Fourier series. *Ann. Sci. ENS*, 45:927–946, 2012. [13](#)
- [27] M. Ben Abid. Prevalent mixed Hölder spectra and mixed multifractal formalism in a product of continuous Besov spaces. *Nonlinearity*, 30:3332–3348, 2017. [38](#)
- [28] M. Ben Slimane. Baire typical results for mixed Hölder spectra on product of continuous Besov or oscillation spaces. *Mediterr. J. Math.*, 13:1513–1533, 2016. [38](#)
- [29] J. Berndsen, A. Lawlor, and B. Smyth. Exploring the wall in marathon running. *J sports Analytics*, 6:173–1860, 1978. [30](#)
- [30] V. Billat, L. Mille-Hamard, Y. Meyer, and E. Wesfreid. Detection of changes in the fractal scaling of heart rate and speed in a marathon race. *Phys. A*, 1997. [31](#)
- [31] V.L. Billat, F. Palacin, M. Correa, and J.R Pycke. Pacing strategy affects the sub-elite marathoner’s cardiac drift and performance. *Front Psychol*, 10:3026, 2020. [30](#)

- [32] V.L. Billat, H. Petot, M. Landrain, R. Meilland, J.-P. Koralsztein, and L. Mille-Hamard. Cardiac output and performance during a 571 marathon race in middle-aged recreational runners. *Sci. World J.*, 19(4):810–859, 2012. [34](#), [49](#)
- [33] F. Broucke and J. Vindas. The pointwise behavior of Riemann’s function. *preprint*, 2021. [12](#)
- [34] G. Brown, G. Michon, and J. Peyrière. On the multifractal analysis of measures. *Journal of Statistical Physics*, 66(3-4):775–790, 1992. [13](#)
- [35] Z. Buczolich and J. Nagy. Hölder spectrum of typical monotone continuous functions. *Real Analysis Exchange*, 26(2):133–156, 2000. [29](#)
- [36] S. Jaffard C. Esser. Divergence of wavelet series: A multifractal analysis. *Adv. in Math.*, 328:928–958, 2018. [13](#)
- [37] A.P. Calderón and A. Zygmund. Local properties of solutions of elliptic partial differential equations. *Studia Math.*, 20:171–223, 1961. [12](#)
- [38] L. Calvet, A. Fisher, and B. Mandelbrot. The multifractal model of asset returns. *Cowles Foundation Discussion Papers: 1164*, 1997. [43](#)
- [39] V. Catrambone, G. Valenza, E. P. Scilingo, N. Vanello, H. Wendt, R. Barbieri, and P. Abry. Wavelet p-leader non-gaussian multiscale expansions for eeg series: an exploratory study on cold-pressor test. In *International IEEE EMBS Conference (EMBC)*, Berlin, Germany, July 2019. [3](#)
- [40] J. Christensen. On sets of Haar measure zero in abelian polish groups. *Israel J. Math.*, 13(3):255–260, 1972. [29](#)
- [41] K. Daoudi, J. Lévy-Véhel, and Y. Meyer. Construction of continuous functions with prescribed local regularity. *Constructive Approximation*, 14:349–385, 1998. [23](#)
- [42] A. Durand. Describability via ubiquity and eutaxy in diophantine approximation. *Ann. Math. Blaise Pascal*, 22:1–149, 2015. [35](#)
- [43] C. Esser and L. Loosveld. Slow, ordinary and rapid points for gaussian wavelets series and application to fractional brownian motions. *Preprint*, 2021. [9](#)
- [44] K. Falconer. *Fractal Geometry: Mathematical Foundations and Applications*. John Wiley & Sons, West Sussex, England, 1993. [35](#)
- [45] A.-H. Fan, L. Liao, and M. Wy. Multifractal analysis of some multiple ergodic averages in linear cookie-cutter dynamical systems. *Mathematische Zeitschrift*, 290:63–81, 2018. [13](#)
- [46] A.H. Fan, L. Liao, and J.-H. Ma. Level sets of multiple ergodic averages. *Monatshefte für Mathematik*, 168:17–26, 2012. [13](#)

- [47] P. Flandrin. *Explorations in Time-Frequency Analysis*. Cambridge University Press, 2018. [19](#)
- [48] Pierre Frankhauser. The fractal approach. a new tool for the spatial analysis of urban agglomerations. *Population: an english selection*, pages 205–240, 1998. [3](#)
- [49] A. Fraysse. Regularity criteria of almost every function in a Sobolev space. *Journal of Functional Analysis*, pages 1806–1821, 2010. [30](#)
- [50] A. Fraysse and S. Jaffard. How smooth is almost every function in a Sobolev space? *Revista Matemática Iberoamericana*, 22(2):663–682, 2006. [29](#)
- [51] U. Frisch. *Turbulence, the Legacy of A.N. Kolmogorov*. Addison-Wesley, 1993. [22](#)
- [52] R. Galaska, D. Makowiec, A. Dudkowska, A. Koprowski, K. Chlebus, J. Wdowczyk-Szulc, and A. Rynkiewicz. Comparison of wavelet transform modulus maxima and multifractal detrended fluctuation analysis of heart rate in patients with systolic dysfunction of left ventricle. *Annals of Noninvasive Electrocadiology*, 13(2):155–164, 2008. [11](#)
- [53] P.C. Ivanov, L.A. Nunes Amaral, A.L. Goldberger, S. Havlin, M.G. Rosenblum, Z.R. Struzik, and H.E. Stanley. Multifractality in human heartbeat dynamics. *Nature*, 399:461–465, 1999. [31](#)
- [54] S. Jaffard. Construction de fonctions multifractales ayant un spectre de singularités prescrit. *Comptes Rendus de l’Académie des Sciences*, 315(5):19–24, 1992. [23](#)
- [55] S. Jaffard. Functions with prescribed Hölder exponent. *Applied and Computational Harmonic Analysis*, 2:400–401, 1995. [23](#)
- [56] S. Jaffard. The spectrum of singularities of Riemann’s function,. *Rev. Mat. Iberoamericana*, 12:441–460, 1996. [12](#)
- [57] S. Jaffard. Multifractal formalism for functions. *SIAM J. of Math. Anal.*, 28(4):944–998, 1997. [5](#), [16](#)
- [58] S. Jaffard. The multifractal nature of Lévy processes. *Proba. Theo. Related Fields*, 114(2):207–227, 1999. [28](#), [35](#)
- [59] S. Jaffard. Construction of functions with prescribed Hölder and chirps exponents. *Revista Matemática Iberoamericana*, 16(2):331–349, 2000. [23](#)
- [60] S. Jaffard. On lacunary wavelet series. *Annals of Applied Probability*, 10(1):313–329, 2000. [35](#)
- [61] S. Jaffard. On the frisch-parisi conjecture. *Journal de Mathématiques Pures et Appliquées*, 79(6):525–552, 2000. [29](#)

- [62] S. Jaffard. On davenport expansions. *Fractal Geometry and Applications: A Jubilee of Benoit Mandelbrot - Analysis, Number Theory, and Dynamical Systems, Pt 1*, 72:273–303, 2004. [5](#)
- [63] S. Jaffard. Wavelet techniques in multifractal analysis. In M. Lapidus and M. van Frankenhuysen, editors, *Fractal Geometry and Applications: A Jubilee of Benoît Mandelbrot, Proc. Symp. Pure Math.*, volume 72(2), pages 91–152. AMS, 2004. [18](#), [24](#), [31](#)
- [64] S. Jaffard. Beyond Besov spaces, part 2: Oscillation spaces. *Constructive Approximation*, 21(1):29–61, 2005. [29](#)
- [65] S. Jaffard. Pointwise regularity associated with function spaces and multifractal analysis. *Banach Center Pub. Vol. 72 Approximation and Probability, T. Figiel and A. Kamont, Eds.*, pages 93–110, 2006. [18](#)
- [66] S. Jaffard. Wavelet techniques for pointwise regularity. *Ann. Fac. Sci. Toul.*, 15(1):3–33, 2006. [18](#)
- [67] S. Jaffard, P. Abry, C. Melot, R. Leonarduzzi, and H. Wendt. Multifractal analysis based on p-exponents and lacunarity exponents. *Fractal Geometry and Stochastics V, C. Bandt et al., Eds., Series Progress in Probability, Birkhäuser*, 70:279–313, 2015. [20](#), [21](#), [22](#), [28](#), [33](#), [38](#), [39](#)
- [68] S. Jaffard, P. Abry, S. Roux, B. Vedel, and H. Wendt. *The contribution of wavelets in multifractal analysis*, pages 51–98. Higher Education Press, Series in contemporary applied mathematics, China, 2010. [10](#), [14](#)
- [69] S. Jaffard, P. Abry, and S.G. Roux. Function spaces vs. scaling functions: tools for image classification. *Mathematical Image processing (Springer Proceedings in Mathematics) M. Bergounioux ed.*, 5:1–39, 2011. [14](#), [15](#), [18](#)
- [70] S. Jaffard, P. Abry, S.G. Roux, B. Vedel, and H. Wendt. *The contribution of wavelets in multifractal analysis*, pages 51–98. Series in contemporary applied mathematics. World scientific publishing, 2010. [26](#)
- [71] S. Jaffard, B. Lashermes, and P. Abry. Wavelet leaders in multifractal analysis. In *Wavelet Analysis and Applications, T. Qian, M.I. Vai, X. Yuesheng, Eds.*, pages 219–264, Basel, Switzerland, 2006. Birkhäuser Verlag. [10](#)
- [72] S. Jaffard and B. Martin. Multifractal analysis of the Brjuno function. *Inventiones Mathematicae*, 212:109–132, 2018. [12](#)
- [73] S. Jaffard and C. Melot. Wavelet analysis of fractal boundaries. *Communications In Mathematical Physics*, 258(3):513–565, 2005. [18](#)
- [74] S. Jaffard, C. Melot, R. Leonarduzzi, H. Wendt, S. G. Roux, M. E. Torres, and P. Abry. p-exponent and p-leaders, Part I: Negative pointwise regularity. *Physica A*, 448:300–318, 2016. [12](#), [16](#), [21](#), [27](#), [31](#)

- [75] S. Jaffard and Y. Meyer. Wavelet methods for pointwise regularity and local oscillations of functions. *Memoirs of the A.M.S.*, 123(587), 1972. [22](#)
- [76] S. Jaffard, S. Seuret, H. Wendt, R. Leonarduzzi, and P. Abry. Multifractal formalisms for multivariate analysis. *Proc. Royal Society A*, 475(2229), 2019. [35](#), [39](#)
- [77] S. Jaffard, S. Seuret, H. Wendt, R. Leonarduzzi, S. Roux, and P. Abry. Multivariate multifractal analysis. *Applied and Computational Harmonic Analysis*, 46(3):653–663, 2019. [38](#)
- [78] C.R. Johnson, P. Messier, W.A. Sethares, A.G. Klein, C. Brown, A.H. Do, P. Klausmeyer, P. Abry, S. Jaffard, H. Wendt, S. Roux, N. Pustelnik, N. van Noord, L. van der Maaten, E. Potsma, J. Coddington, L.A. Daffner, H. Murata, H. Wilhelm, S. Wood, and M. Messier. Pursuing automated classification of historic photographic papers from raking light photomicrographs. *Journal of the American Institute for Conservation*, 53(3):159–170, 2014. [3](#)
- [79] J.-P. Kahane. *Some random series of functions*. Cambridge University Press, 1985. [9](#), [43](#)
- [80] J. W. Kantelhardt, S. A. Zschiegner, E. Koscielny-Bunde, S. Havlin, A. Bunde, and H. E. Stanley. Multifractal detrended fluctuation analysis of nonstationary time series. *Physica A*, 316(1):87–114, 2002. [10](#)
- [81] A.N. Kolmogorov. The Wiener spiral and some other interesting curves in Hilbert space (russian),. *Dokl. Akad. Nauk SSSR*, 26:(2):115–118, 1940. [9](#)
- [82] A.N. Kolmogorov. The local structure of turbulence in incompressible viscous fluid for very large Reynolds numbers. *Comptes Rendus De L’Academie Des Sciences De L’Urss*, 30:301–305, 1941. [4](#)
- [83] B. Lashermes, S. Jaffard, and P. Abry. Wavelet leader based multifractal analysis. *2005 Ieee International Conference On Acoustics, Speech, and Signal Processing, Vols 1-5*, pages 161–164, 2005. [5](#)
- [84] B. Lashermes, S.G. Roux, P. Abry, and S. Jaffard. Comprehensive multifractal analysis of turbulent velocity using the wavelet leaders. *European Physical Journal B*, 61(2):201–215, 2008. [5](#)
- [85] B. Lashermes, S.G. Roux, P. Abry, and S. Jaffard. Comprehensive multifractal analysis of turbulent velocity using the wavelet leaders. *European Physical Journal B*, 61:201–215, 2008. [10](#)
- [86] R. Leonarduzzi, P. Abry, S. Jaffard, H. Wendt, L. Gournay, T. Kyriacopoulou, C. Martineau, and C. Martinez. P-leader multifractal analysis for text type identification. In *IEEE Int. Conf. Acoust., Speech, and Signal Proces. (ICASSP)*, New Orleans, USA, March 2017. [3](#)

- [87] R. Leonarduzzi, H. Wendt, S. G. Roux, M. E. Torres, C. Melot, S. Jaffard, and P. Abry. p-exponent and p-leaders, Part II: Multifractal analysis. Relations to Detrended Fluctuation Analysis. *Physica A*, 448:319–339, 2016. [11](#), [31](#)
- [88] D. E. Lieberman and D. M. Bramble. The evolution of marathon running: capabilities in humans. *Sports Medicine*, 2007. [30](#)
- [89] T. Lux. Higher dimensional multifractal processes: A gmm approach. *Journal of Business and Economic Statistics*, 26(2):194—210, 2007. [34](#)
- [90] B. Mandelbrot. Geometry of homogeneous scalar turbulence: iso-surface fractal dimensions $5/2$ and $8/3$. *J. Fluid Mech.*, 72(2):401–416, 1975. [3](#)
- [91] B. Mandelbrot. *Fractals and scaling in finance*. Selected Works of Benoit B. Mandelbrot. Springer-Verlag, New York, 1997. Discontinuity, concentration, risk, Selecta Volume E, With a foreword by R.E. Gomory. [43](#)
- [92] B. Mandelbrot and J.W. van Ness. Fractional Brownian motion, fractional noises and applications. *SIAM Reviews*, 10:422–437, 1968. [9](#)
- [93] S. Marmi, P. Moussa, and J.C. Yoccoz. The Brjuno functions and their regularity properties. *Comm. Math. Phys.*, 186(2):265–293, 1997. [12](#)
- [94] M. Maron, S.M Horvath, J.E. Wilkerson, and J.A. Gliner. Oxygen uptake measurements during competitive marathon runnings. *J. Appl. Physiol.*, 10:137–150, 1978. [30](#), [31](#)
- [95] P. Mattila. *Geometry of Sets and Measures in Euclidian Spaces*. Cambridge University Press, 1995. [35](#)
- [96] C. Meneveau, K.R. Sreenivasan, P. Kailasnath, and M.S. Fan. Joint multifractal measures - theory and applications to turbulence. *Physical Review A*, 41(2):894–913, January 1990. [6](#), [37](#), [38](#)
- [97] Y. Meyer. *Ondelettes et Opérateurs*. Hermann, Paris, 1990. English translation, *Wavelets and operators*, Cambridge University Press, 1992. [14](#), [16](#), [18](#)
- [98] Y. Meyer. *Wavelets, vibrations and scalings*. CRM Ser. AMS Vol. 9,, Presses de l’Université de Montréal, Paris, 1998. [10](#), [31](#)
- [99] J.F. Muzy, E. Bacry, and A. Arneodo. Wavelets and multifractal formalism for singular signals: application to turbulence data. *Phys. Rev Lett.*, 67:3515–3518, 1991. [5](#), [10](#)
- [100] G. Parisi and U. Frisch. Fully developed turbulence and intermittency. In M. Ghil, R. Benzi, and G. Parisi, editors, *Turbulence and Predictability in geophysical Fluid Dynamics and Climate Dynamics*, Proc. of Int. School, page 84, Amsterdam, 1985. North-Holland. [5](#), [29](#)

- [101] J. Peyrière. A vectorial multifractal formalism. *Proc. Symp. Pure Math.*, 72.2(2):217–230, 2004. [6](#), [38](#)
- [102] Jean-Renaud Pycke and Véronique Billat. Marathon performance depends on pacing oscillations between non symmetric extreme values. *International Journal of Environmental Research and Public Health*, 19(4):2463, 2022. [30](#), [34](#)
- [103] R.H. Riedi. Multifractal processes. In P. Doukhan, G. Oppenheim, and M.S. Taqqu, editors, *Theory and applications of long range dependence*, pages 625–717. Birkhäuser, 2003. [47](#)
- [104] G. Saes. Sommes fractales de pulses : Etude dimensionnelle et multifractale des trajectoires et simulations. *PhD Thesis of University Paris Est Creteil*, 2021. [22](#), [28](#)
- [105] S. Seuret. On multifractality and time subordination for continuous functions. *Adv. Math.*, 220(3):936–963, 2009. [47](#)
- [106] S. Seuret. A survey on prescription of multifractal behaviors. *Fractal geometry and stochastics 6, to appear*, 2022. [23](#)
- [107] S. Seuret and J. Lévy-Véhel. The 2-microlocal formalism. *Fractal Geometry and Applications: A Jubilee of Benoit Mandelbrot - Analysis, Number Theory, and Dynamical Systems, Part 2*, 72:153–215, 2004. [20](#)
- [108] S. Seuret and A. Ubis. Local l^2 -regularity of riemann’s fourier series. *Annales de l’Institut Fourier*, 67:2237–2264, 2017. [12](#)
- [109] F. Sémécurbe, C. Tannier, and S.G. Roux. Spatial distribution of human population in france: exploring the MAUP using multifractal analysis. *Geographical Analysis*, 48:292–313, 2016. [3](#)
- [110] B. Smyth. Fast starters and slow finishers: A large-scale data analysis of pacing at the beginning and end of the marathon for 579 recreational runners. *J Sports Analytics*, 4:229–242, 2018. [30](#)
- [111] B. Smyth. How recreational marathon runners hit the wall : A large-scale data analysis of late-race pacing collapse in the 577 marathon. *PLoS One*, 16:578, 2022. [30](#)
- [112] H. Wang, L. Xiang, and R. B. Pandey. A multifractal detrended fluctuation analysis (MDFA) of the Chinese growth enterprise market (GEM). *Physica A*, 391(12):3496 – 3502, 2012. [11](#)
- [113] H. Wendt, P. Abry, and S. Jaffard. Bootstrap for empirical multifractal analysis. *IEEE Signal Processing Mag.*, 24(4):38–48, 2007. [18](#)
- [114] E. Wesfreid, V. Billat, and Y. Meyer. Multifractal analysis of heartbeat time series in human races. *Appl. Comput. Harmon. Anal.*, 2010. [31](#)

- [115] B. Whitcher, P. Guttorp, and D.B. Percival. Wavelet analysis of covariance with application to atmospheric time series. *J. Geophys. Res. Atmos.*, page 14941–14962, 2000. [36](#)
- [116] J. Lindenstrauss Y. Benyamini. *Geometric Nonlinear Functional Analysis*. Colloquium publications (American Mathematical Society, Providence, Rhode Island, 2000. [29](#)